RESEARCH DEPARTMENT

Shaping the vertical radiation patterns of v.h.f. and u.h.f. transmitting aerials by phase perturbation

RESEARCH REPORT No. E-121

UDC 621.396.677.31 1966/72

THE BRITISH BROADCASTING CORPORATION
ENGINEERING DIVISION

RESEARCH DEPARTMENT

SHAPING THE VERTICAL RADIATION PATTERNS OF V.H.F. AND U.H.F. TRANSMITTING AERIALS BY PHASE PERTURBATION

Research Report No. E-121
UDC 621.396.677.31 1966/72

P.C.J. Hill, Ph.D.,B.Sc.,D.I.C.,Grad.I.E.E.

D. Maurice
for Head of Research Department

This Report is the property of the British Broadcasting Corporation and may not be reproduced in any form without the written permission of the Corporation.

This Report uses SI units in accordance with B.S. document PD 5686.

Research Report No. E-121

SHAPING THE VERTICAL RADIATION PATTERNS OF V.H.F. AND U.H.F. TRANSMITTING AERIALS BY PHASE PERTURBATION

Section Title Page

SUMMARY 1

LIST OF PRINCIPAL SYMBOLS 1

1. INTRODUCTION 1

2. THE SYNTHESIS PROBLEM AND ITS SOLUTION 3

2.1. Formal Solutions 3
2.2. Basic Principles of the Phase Perturbation Method 4

3. SYNTHESIS TECHNIQUES FOR THE PHASE PERTURBATION METHOD 5

3.1. General Considerations 5
3.2. Synthesis of the Quadrature Pattern 7
3.3. Non-oscillatory Solution 8
3.4. Oscillatory Solution 10
3.5. Relation Between Solutions 13

4. APPLICATION TO U.H.F. TRANSMITTING AERIALS 14

4.1. Aerials with Individually-fed Tiers 14
4.2. Panel Aerials 15
4.3. Impedance, Gain Reduction and Bandwidth 18

5. MISCELLANEOUS CONSIDERATIONS 20

5.1. The Effects of Inter-tier Mutual Coupling 20
5.2. Random Phase Errors 21

6. FINAL REMARKS AND CONCLUSIONS 22

7. REFERENCES 23

8. APPENDIX 24

December, 1966.
Research Report No. E-121
UDC 621.396.677.31 1966/72

SHAPING THE VERTICAL RADIATION PATTERNS OF V.H.F AND U.H.F. TRANSMITTING AERIALS BY PHASE PERTURBATION

SUMMARY

An important consideration arising in the design of v.h.f. and u.h.f. transmitting aerials is the provision of a vertical radiation pattern which gives uniform field strength over the prescribed service area. An adequate solution is provided by a beam-tilted "cosecant" radiation pattern. Methods are described for synthesizing radiation patterns of this type by varying the phases of the radiating currents in a constant amplitude linear array of equi-spaced elements. Some examples are given of the application of these techniques to the types of multi-tier aerial employed at v.h.f. and u.h.f. broadcast stations. Finally, the problem of actually achieving the prescribed current distributions and radiation patterns in the presence of inter-tier mutual coupling and random phase errors is briefly discussed.

LIST OF PRINCIPAL SYMBOLS

α	parameter defined in Section 5.2.
A	aerial aperture (wavelengths)
d	"fundamental" spacing between elements
D	distance between transmitting and receiving aerials
$\hat{E}$	amplitude of main lobe
g	gain reduction due to null-filling (dB)
g_k	specified null-filling amplitude at the k^{th} null-point
I_r	complex current in the r^{th} element
k	null-point number
l_r	length of r^{th} branch feeder
L	mean length of branch feeders
m	null-filling index
M	number of panels
n	number of dipoles per panel
N	total number of elements in array
q	spacing of dipole from screen
r	number of element in array
R_0	characteristic impedance of branch feeder
s	dipole spacing (wavelengths)
v	parameter defined in Section 5.2.
V_0	common driving-point voltage at branch feeder junction
x	distance along continuous array (wavelengths)
x_r	horizontal stagger of r^{th} element (wavelengths)
Z_{rq}	mutual impedance between r^{th} and q^{th} dipoles
β	phase constant
δ	corrective phase perturbation for oscillatory solution
Δ	half the differential phase shift between array halves, non-oscillatory solution
ε_r	phase error in r^{th} branch feeder
λ	wavelength
σ	standard deviation of phase distribution ϕ_r
σ_ε	standard deviation of random phase errors ε_r
θ	angle below the horizontal line
θ_0	beam-tilt angle
ρ	reflexion coefficient
ρ_{in}	input reflexion coefficient of aerial
ϕ_r	phase perturbation of r^{th} element, symmetrical distribution
ϕ_0	linear phase progression, radians/tier (upwards)
Φ_r	total phase perturbation of r^{th} element
ψ	parameter defined in Equation (1)

1. INTRODUCTION

An ideal broadcast service provides uniform field strength at all distances up to the limit of the service area. Practical aerials cannot easily satisfy this requirement in the more distant parts of the service area because path attenuation increases rapidly as the horizon is approached. It is possible, however, to shape the vertical radiation pattern (v.r.p.) of an aerial in order to achieve approximately uniform field strength near to the transmitter, especially at u.h.f. where it is found experimentally that the average received field strength is approximately equal to that of the direct wave because local ground irregularity reduces the contribution from the ground-reflected wave to an insignificant level.

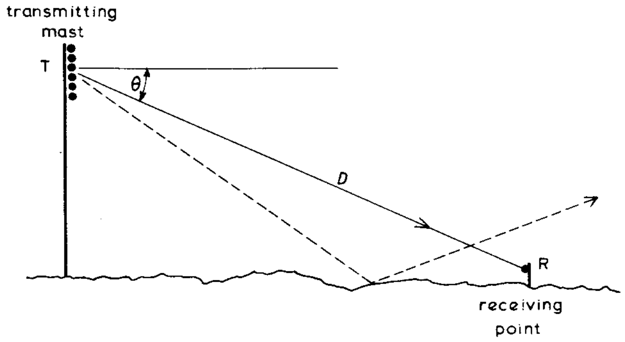

Fig. 1 - Ultra-high-frequency transmission - basic geometry

The v.r.p. which is required to achieve uniform direct-wave field strength is easily derived. Referring to Fig. 1, the average field strength at R due to an isotropic aerial at T is proportional to $1/D$ and therefore to $\sin\theta$, where θ is the inclination angle of TR. It follows therefore that an aerial whose v.r.p. is proportional to $\operatorname{cosec}\theta$ will produce a uniform average field strength in the nearer parts of the service area, where earth curvature may be neglected.

The simplest form of transmitting aerial consists of a vertical array of up to 40 similar tiers of elements, each carrying equal co-phased currents. Provided the inter-tier spacing does not exceed one wavelength (1·0λ) the v.r.p. in the important region, $0 < \theta < \pi/6$, is given approximately by

$$E(\theta) \simeq \frac{\sin\psi}{\psi} \qquad (1)$$

where $\psi = \pi A \sin\theta$

and A is the aerial aperture in wavelengths. The magnitude of this pattern $|E(\theta)|$ is plotted as a function of ψ in Fig. 2(*a*). The envelope of the curve is given by $1/\psi$ and since this is proportional to $\operatorname{cosec}\theta$, it follows that the envelope represents the v.r.p. which gives uniform field strength in the nearer parts of the service area. Thus, if the nulls between the lobes can be filled to approach the level of this envelope, the v.r.p. would be approximately equal to a $\operatorname{cosec}\theta$ pattern over a wide range of angles. This process, known as "null-filling", is not required above the horizontal (ψ negative in Fig. 2(*a*)); consequently an optimum null-filling procedure would involve taking the energy from the lobes in the upper part of the pattern and placing it in the gaps between the lobes in the lower part.

The beamwidth of the main lobe of a u.h.f. aerial is typically very narrow; a 40λ-aerial, for example, has a half-power beamwidth of only 1·3°. If such an aerial were mounted at the top of a tall mast the horizon angle will be comparable with the beamwidth of the main lobe and there would be a reduction of effective radiated power (e.r.p.) at the horizon unless this lobe were tilted downwards by a small angle. The precise value of tilt angle which gives the most uniform field strength within a given service area depends upon the height and aperture of the transmitting aerial[1]; in general, however, the main lobe should be aimed at the limit of the service area. As an example, an aerial mounted 300 m (1000 ft) above ground should have its main lobe tilted downwards by approximately 0·5° to serve an area up to a distance of 56 km (35 miles).

The v.r.p. which is required for a u.h.f. service is therefore one which is beam-tilted and null-filled below the horizontal. A typical specification is written as:

$$|E(\theta)| \nless \frac{m\hat{E}\operatorname{cosec}(\theta - \theta_0)}{\pi A} \qquad \sin^{-1}\frac{1}{2A} < \theta - \theta_0 < \pi/6 \qquad (2)$$

where $\hat{E}$ is the amplitude of the main lobe, θ_0 the beam-tilt and m is defined as the null-filling index.*

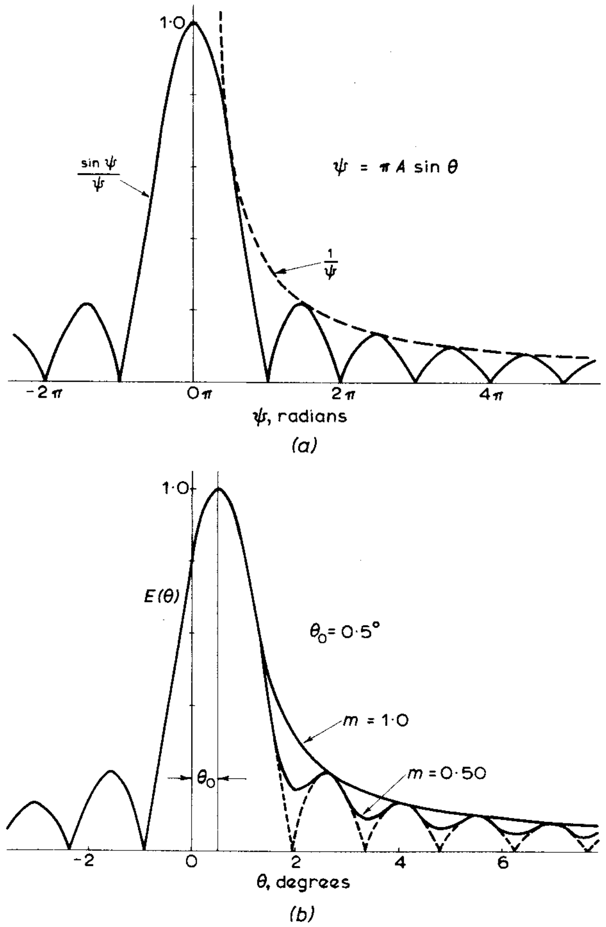

(*a*)

(*b*)

Fig. 2 - The null-filling problem:

(*a*) vertical radiation pattern of a uniform array
(*b*) idealized vertical radiation patterns for a 40λ-array with 0·5° beam-tilt

---

* 100 m is often referred to as the "percentage null-filling".

The shape of the pattern above the horizon ($-\pi/2 < \theta < 0$) is generally unimportant providing the desired aerial gain can be achieved. Idealized vertical radiation patterns are shown in Fig. 2(*b*) for a 40λ-aerial with a beam-tilt of 0·5° and null-filling indices $m = 0{\cdot}50$ and $m = 1{\cdot}0$.

In this report we describe methods for synthesizing radiation patterns of the type described by Equation (2) by constructing suitable phase distributions across the aperture of a constant amplitude equispaced linear array. This arrangement is advantageous from a practical standpoint because it may be simply and economically achieved by energizing tiers of identical groups (or panels) of elements through branch feeders of slightly different electrical lengths.

At v.h.f. fewer tiers of elements are used and broader main lobes result. Consequently beam-tilt is seldom necessary and null-filling is only required if the aerial is situated near a built-up area. Although the synthesis methods described are equally valid for v.h.f. and u.h.f. aerials, emphasis is placed on their application to u.h.f. aerials throughout the report.

2. THE SYNTHESIS PROBLEM AND ITS SOLUTION

The problem is to synthesize a cosecant radiation pattern with a lower bound given by Equation (2) as accurately as possible from a linear array of discrete sources occupying a fixed aperture. Restricting attention to apertures of constant amplitude the preferred arrangements of sources, in order of preference, are:

(*a*) Equally spaced sources or tiers carrying currents of equal amplitude but arbitrary phase

(*b*) Unequally spaced sources carrying equal co-phased currents

(*c*) Unequally spaced sources carrying currents of equal amplitude but arbitrary phase

Subsidiary requirements are that the aperture distribution should not vary appreciably with frequency and that each half of the aerial should have a v.r.p. which is satisfactory for emergency use.

2.1. Formal Solutions

Let us consider a linear array of N equally spaced isotropic radiating elements with an aperture distribution given by $I(r)$, the set of element currents. The complex radiation pattern $p(\sin\theta)$ of the array may be written

$$p(\sin\theta) = \sum_r I(r)\varepsilon^{-j\beta dr\sin\theta} \qquad (3)$$

where dr is the distance of element r from the point of phase reference, d the "fundamental" spacing of the elements and β the phase constant ($= 2\pi/\lambda$) with λ the wavelength. In this expression, $I(r)$ will be recognized as the complex line spectrum[2] of the pattern function $p(\sin\theta)$ so that from the Fourier transform theorem we may write

$$I(r) = \frac{d}{\lambda}\int_{-\lambda/2d}^{\lambda/2d} p(\sin\theta)\varepsilon^{j\beta dr\sin\theta}\, d\sin\theta \qquad (4)$$

Formally, the solution to the synthesis problem is given by the integral transform of $p(\sin\theta)$ in Equation (4). The complex pattern $p(\sin\theta)$ repeats every λ/d in $\sin\theta$ and its control is confined to this region through the $2N - 1$ degrees of freedom within the aperture distribution. Thus the accuracy with which a pattern may be synthesized can be increased for a given aperture by increasing N and reducing d, but the pattern enters the imaginary region ($\sin\theta > 1$) if d is less than $\lambda/2$. This means that the limiting accuracy of a synthesized pattern is set by the amount of reactive energy which can be tolerated within the aperture[3]; moreover, mutual effects between elements preclude the actual realisation of a very closely spaced distribution.

Direct evaluation of Equation (4) is impossible in all but a few special cases, particularly as we are normally only concerned with the power pattern, $p(\sin\theta)\,p(\sin\theta)^*$, so that the phase variation of the complex pattern becomes arbitrary. If the power pattern is used in place of $p(\sin\theta)$ in Equation (4) and the integral transform taken, then by the autocorrelation theorem[2] we derive the autocorrelation function of the original distribution $I(r)$, thereby transferring the arbitrariness of the complex pattern to the aperture distribution. An explicit solution to the synthesis problem is therefore impossible in general; in the present case, the problem is further complicated because we are imposing the constraint of a constant amplitude aperture distribution in addition to limiting the size of the aperture itself. The aperture limitation may be satisfied by synthesizing the required pattern from a set of aperture-limited functions which are orthogonal and complete on the $\sin\theta$ axis, the best known example being Woodward's "sinc" function (Equation (1)).** The inclusion of constraints in the problem suggests the use of variational methods.

In the now classic paper of Woodward,[4] a co-phased cosecant radiation pattern is synthesized from a set of shifted sinc functions to give a complex aperture distribution which is even in amplitude and odd in phase. In theory, this solution could be adapted to an arrangement of unequally-spaced sources carrying currents of equal amplitude with an appropriate phase distribution.

* The asterisk denotes the complex conjugate.

** Woodward's sinc function is defined by

$$\operatorname{sinc} x = \frac{\sin \pi x}{\pi x}$$

A variational approach to the general problem of pattern synthesis has been made by a few workers. Harris and Shanks[5] deal with the synthesis of directional patterns for a source distributed over a radiating surface of arbitrary shape, maximising the power density in a specified direction if the source is limited in magnitude and extent. Rhodes[6] describes a method for achieving the best mean-square approximation to a specified radiation pattern from a line source of arbitrary length by employing special aperture-limited functions which are complete within the real part of the sin θ axis. Finally, in a paper by Proctor and Ablow,[7] a procedure is given for optimising a synthesized power pattern from a limited aperture, a predetermined compromise being made between mean-square pattern error and aperture function "smoothness". Variational methods suffer from the disadvantage that rather arbitrary decisions must be taken at the outset.

For very large apertures, geometrical-optics techniques may be applied and the "stationary phase" method of solving the radiation pattern integral as described by Dunbar[8] and Shanks[9] can be extended to the case of an aperture of constant amplitude. For the relatively small apertures under consideration, however, such a method requires further perturbation of the resultant phase distribution for accurate synthesis of uniformly null-filled radiation patterns.

In the present problem, the variational approach has been rejected in favour of a method which takes advantage of the fact that the radiation pattern of a uniform array may be made to approach the required cosecant pattern (Equation (2)) by filling in the nulls between the pattern side-lobes. If the null-filling energy can be supplied without unduly perturbing the shape of the original pattern the constant amplitude requirement may be satisfied with a uniformly spaced array. The basic principles of the method are described below

2.2. Basic Principles of the Phase Perturbation Method

The radiation pattern of a uniform distribution of N (even) isotropic sources spaced $1{\cdot}0\lambda$ apart* is given by Equation (3) as

$$p_0(\sin\theta) = \frac{\sin(N\pi\sin\theta)}{\sin(\pi\sin\theta)} \qquad (5)$$

and the starting point of the method is the observation that the envelope of this pattern closely follows the function $(1/\pi)\operatorname{cosec}\theta$ over the range $-0{\cdot}25 < \sin\theta < 0{\cdot}25$. We note that this "primary" pattern (Equation (5)) is co-phased and real. A co-phased "secondary" distribution is selected to give the required null-filling radiation pattern and then added in phase-quadrature to the primary (uniform) distribution so that the null-filling pattern is itself in quadrature with the primary pattern. The secondary distribution and its pattern must both be even functions** since it follows from Equations (3) and (4) that this condition will make them jointly co-phased. A small correction is then made to the primary distribution in order to make the resultant equal in amplitude to the original primary distribution. The reason for choosing the primary and secondary distributions (and patterns) to be orthogonally phased is to make their specification initially independent and also to greatly simplify the correction required to meet the constant amplitude condition. The process is illustrated vectorially in Fig. 3(*a*). In general, further correction must be made to remove the errors which are introduced by null-filling a primary pattern which is subsequently modified to maintain the constant amplitude condition. In practice, the accuracy of the null-filling synthesis and pattern correction is checked by radiation pattern computation.

Two solutions are available for the secondary distribution. The first is a non-oscillatory function (Fig. 3(*b*)) which has a pattern amplitude equal to that of the required cosecant pattern at each null-point of the primary pattern; with this solution, error correction becomes particularly simple in practice as it involves only the single step of introducing a differential phase-shift between the upper and lower halves of the array. The second solution is an oscillatory function (Fig. 3(*c*)) which again satisfies the cosecant pattern specification at the primary null-points but with amplitudes which alternate in sign at successive points. Such a function possesses the advantage of crossing the sin θ axis near the points where the primary pattern achieves its maximum amplitudes, with the result that subsequent pattern correction is not required provided this condition is maintained.

To summarize, the procedure for synthesizing a cosecant radiation pattern by the phase perturbation method is to:

(i) fill the nulls of the pattern $p_0(\sin\theta)$ which occur at $\sin\theta = 1/N,\ 2/N,\ 3/N, \ldots\ldots\ldots.,$ with a suitably constructed co-phased pattern placed in phase quadrature with the original or primary (in-phase) pattern.

(ii) synthesize the secondary or quadrature pattern with a co-phased distribution even in amplitude

(iii) modify the primary distribution to satisfy the constant amplitude requirement for the total distribution

---

* There is no loss of generality in making $d/\lambda = 1$ since the general case is obtained by re-scaling the sin θ axis by the factor λ/d.

** $p(\sin\theta) = p(-\sin\theta)$ and $I(r) = I(-r)$.

(iv) adjust the resultant distribution to remove the errors introduced by null-filling the unmodified primary pattern

(v) achieve the desired beam-tilt by shifting the resultant pattern on the sin θ axis with a superimposed linear phase distribution

(vi) compute the radiation pattern to check the resultant null-filling.

The method of synthesis will now be described in greater detail.

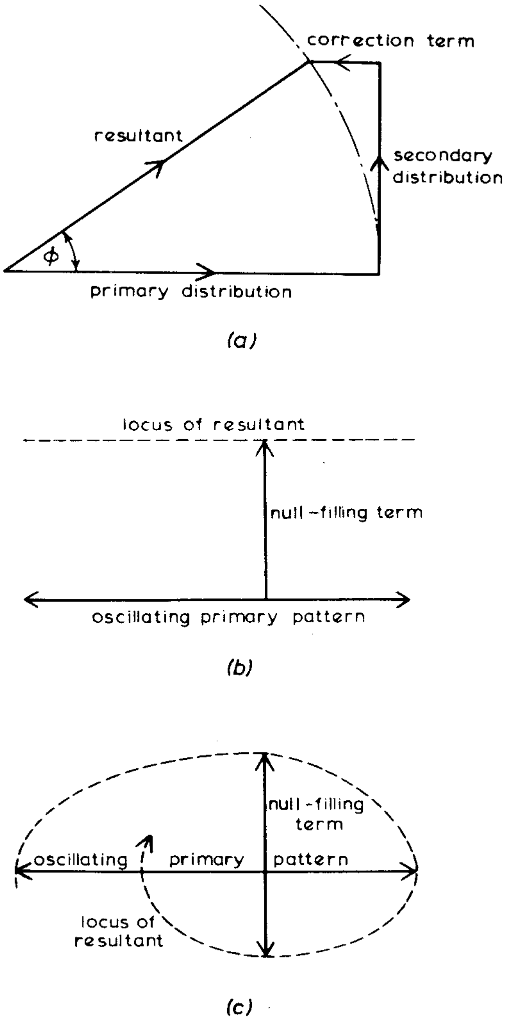

Fig. 3 - Vector representation of null-filling by the phase perturbation method

(*a*) typical point on aperture distribution
(*b*) radiation pattern in side-lobe region - non-oscillatory solution
(*c*) radiation pattern in side-lobe region - oscillatory solution

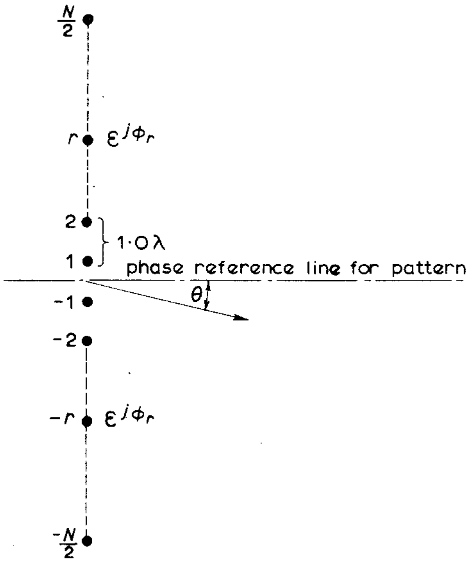

Fig. 4 - Array of N isotropic sources spaced 1·0λ apart with an even phase distribution ϕ_r

3. SYNTHESIS TECHNIQUES FOR THE PHASE PERTURBATION METHOD

3.1. General Considerations

In the phase perturbation method, the quadrature distribution required for null-filling and its corresponding radiation pattern are both even functions so that the resultant phase distribution must be an even function also. The primary radiation pattern $p_0(\sin\theta)$ of a uniform array of N (even) sources spaced 1·0λ apart has been given by Equation (5). The component of this pattern due to the r^{th} pair of sources (Fig. 4) is $2\cos(\overline{2r-1}\,\pi\sin\theta)$. If their phases are perturbed symmetrically by ϕ_r radians, a quadrature component of amplitude $\sin\phi_r$ and an in-phase error component of amplitude $(\cos\phi_r - 1)$ are added to the primary pattern. If the phase shift ϕ_r is a small departure from the equi-phased condition these amplitudes become ϕ_r and $-\phi_r^2/2$ respectively to a second order approximation. It follows that an even phase perturbation over the array, ϕ_r, yields a resultant pattern $p(\sin\theta)$ which may be written as

$$p(\sin\theta) \simeq p_0(\sin\theta) + j2\sum_{r=1}^{N/2}\phi_r\cos(\overline{2r-1}\,\pi\sin\theta) - \sum_{r=1}^{N/2}\phi_r^2\cos(\overline{2r-1}\,\pi\sin\theta) \qquad (6)$$

where $p_0(\sin\theta)$ is given by Equation (5). The second term on the right hand side of Equation (6) is the quadrature pattern available for null-filling and the last term is the net primary error pattern due to phase perturbation.

The number of degrees of freedom in ϕ_r has been limited to $N/2 - 1$ because the sources have been perturbed symmetrically in pairs. This means that the quadrature pattern may be specified independently at $N/2 - 1$ points. These points are conveniently chosen to be the null points of $p_0(\sin\theta)$, occurring at $\sin\theta = 1/N, 2/N, 3/N, \ldots\ldots$, where it is required that the amplitude of the resultant pattern must not fall below that given by Equation (2). When θ_0, the beam-tilt angle, is very small it is sufficiently accurate to rewrite Equation (2) as,

$$|p(\sin\theta)| \nless \frac{m}{\pi(\sin\theta - \sin\theta_0)} \qquad (7)$$

where A has been replaced by N (source spacing $1{\cdot}0\lambda$) and $\hat{E}$, the amplitude of the main lobe, has been equated to N also on the basis that the null-filling will result in only a very small reduction in the amplitude of the main lobe.

Equation (7) shows that, at this stage in the procedure, we may conveniently set $\theta_0 = 0$ and achieve the desired beam-tilt by shifting the resultant null-filled pattern on the $\sin\theta$ axis as a final step. The linear phase progression required for a beam-tilt angle θ_0 is given by

$$\phi_0 = \frac{2\pi d\theta_0}{\lambda}\ \text{radians/tier} \qquad (8)$$

for an inter-tier spacing of d.

The quadrature pattern is given, from Equation (7), as a set of null-filling amplitudes $g_k = m/\pi\sin\theta$ with $\sin\theta = 1/N, 2/N, \ldots\ldots k/N, \ldots\ldots (N/2 - 1)/N$. This process is illustrated in Fig. 5 for a typical specification of $m = 0{\cdot}50$, for θ lying between the half-amplitude point of the main lobe and $\theta = \pi/12$ and $m = 0{\cdot}25$, for $\pi/12 < \theta < \pi/6$. It should be noted that the null at $\sin\theta = 0{\cdot}5$ will remain unfilled with a symmetrical distribution, since every pair of sources will have a zero in this direction. In general this unfilled null will appear at $\sin\theta = \lambda/2d$.

Another result of the distribution symmetry is that the $N/2 - 1$ nulls above the horizontal are also filled and consequently those nulls beyond $\sin\theta = 0{\cdot}5$ are filled, since this part of the pattern is a repeat of the pattern in the range $-0{\cdot}5 < \sin\theta < 0$. It follows therefore that, although the pattern cannot be specified beyond $\sin\theta = 0{\cdot}5$, in general the null-filling in this region will be quite satisfactory.

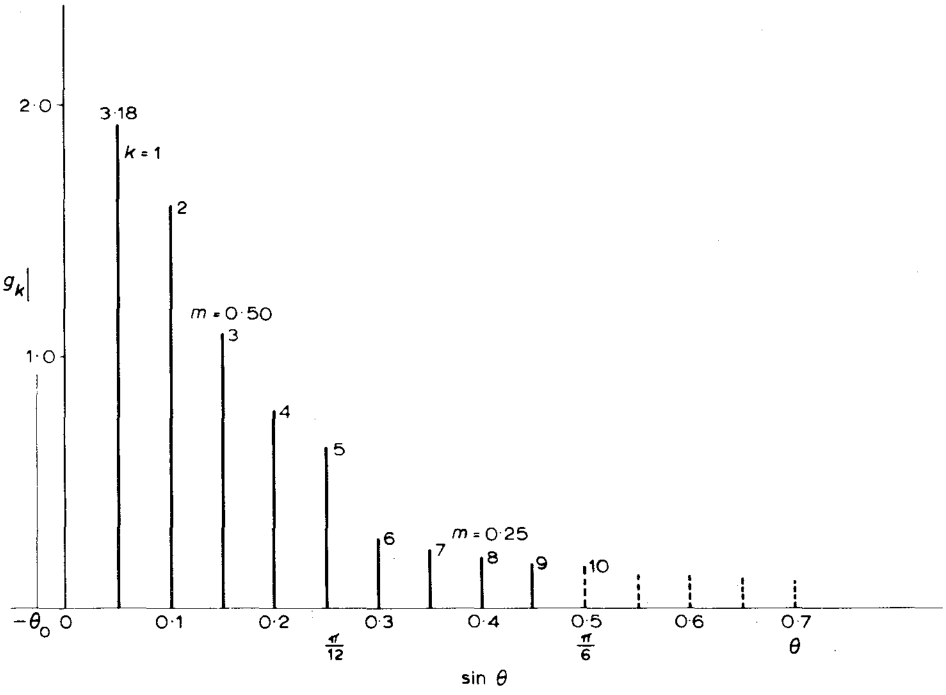

Fig. 5 - Typical specification of quadrature pattern in the nulls of the primary pattern for a 20λ-array, $g_k = mN/\pi k$, *$m = \theta{\cdot}50$ and $0{\cdot}25$*

3.2. Synthesis of the Quadrature Pattern

Two methods are available for synthesizing the quadrature pattern.

In the direct method the expression for the quadrature pattern (the second term on right hand side of Equation (6)) is equated to the null-filling specification at the null points of the primary pattern. The phase distribution ϕ_r of the outer $N/2 - 1$ pairs of sources is determined from the set of equations

$$\sum_{r=1}^{N/2} \phi_r \cos(\overline{2r-1}\,\pi \sin\theta) = \pm\frac{m}{2\pi\sin\theta}$$

$$= \frac{g_k}{2} \qquad (9)$$

$$\text{where } \sin\theta = \frac{1}{N}, \frac{2}{N}, \ldots\ldots \frac{k}{N}, \ldots\ldots \frac{N/2-1}{N}$$

The innermost pair of elements ($r = 1$, Fig. 4) may be taken as the phase reference for the array, i.e. $\phi_1 = 0$. The sign on the right hand side of each Equation (9) depends on the type of solution to be adopted; in the non-oscillatory case all the signs are identical and in the oscillatory case the sign is made to alternate in consecutive equations. This synthesis method, although direct, may involve a prohibitive number of variables if the array is very large. A 40λ-array, for example, would involve the solution of a 19 × 19 matrix in its quadrature pattern synthesis. The alternative method is normally more convenient to use in practice.

The second method depends on the fact that a continuous aperture distribution may be closely simulated by an array of suitably spaced point sources. The continuous quadrature distribution is synthesized from $N/2 - 1$ pairs of shifted sinc pattern functions which fill pairs of zeros, equally spaced above and below the horizontal, with amplitudes given by the null-filling specification $mN/\pi k$. Each pair of sinc functions independently satisfies the null-filling requirement at its position on the $\sin\theta$ axis and its contribution to the continuous distribution is an even, quadrature, aperture-limited function as required. The mechanism is illustrated in Fig. 6 for the k^{th} null-point. Formally, the analytical steps are as follows. A unit amplitude sinc function, $\text{sinc}(\sin\theta)$ ($= \sin(\pi\sin\theta)/\pi\sin\theta$) transforms to a unit amplitude rectangular function $F(x)$, where x is in wavelengths and $F(x) = 1$ for $-\frac{1}{2} \leqslant x \leqslant \frac{1}{2}$ and is zero outside those limits. An aperture distribution N wavelengths wide and uniformly illuminated $F(x/N)$ therefore gives a pattern function $N\,\text{sinc}(N\sin\theta)$. It follows that a null-filling component of amplitude g_k placed at the origin ($\sin\theta = 0$) will be provided by a distribution $(g_k/N)F(x/N)$. Finally, beam-tilts of $\pm k/N$ in $\sin\theta$ will modulate the rectangular distribution by $\varepsilon^{\pm j2\pi kx/N}$ so that the even pairs of null-filling components transform in combination to a distribution $f(x)$ given by

$$f(x) = \sum_{k=1}^{N/2}\left(\frac{2g_k}{N}\right)\cos\left(\frac{2\pi kx}{N}\right)F\left(\frac{x}{N}\right) \qquad (10)$$

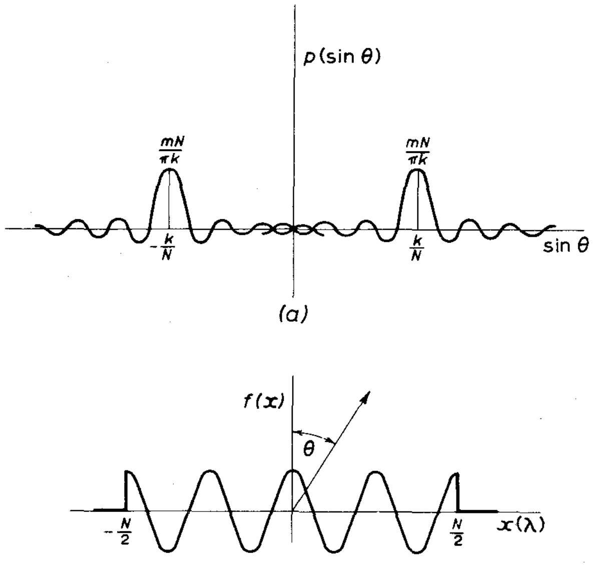

Fig. 6 - Aperture limited distribution corresponding to a pair of shifted sinc patterns
(*a*) pattern (*b*) distribution

Equation (10) is an expression for the continuous quadrature distribution which is to be simulated by a point source array. For a spacing of 1·0λ, sources are placed at $x = \pm\frac{1}{2}, \pm 3/2, \pm 5/2, \ldots\ldots \pm(N-1)/2$; their amplitudes are normally given by Equation (10) although in some cases it is more accurate to plot Equation (10) and take mean integrated samples for the equivalent discrete distribution. For the r^{th} pair of sources $x = (2r-1)/2$ and if $g_k = mN/\pi k$ is inserted into Equation (10) we obtain a simple explicit formula for the quadrature current in the r^{th} pair of sources for direct sampling at 1·0λ intervals. Their phase perturbation ϕ_r is therefore given by

$$\phi_r \simeq \sum_{k=1}^{N/2}\left(\pm\frac{2m}{\pi k}\right)\cos\left(\frac{\overline{2r-1}\,\pi k}{N}\right) \qquad (11)^*$$

Again, the signs on the right hand side of Equation (11) depend on whether the oscillatory or non-oscillatory solution is employed and it is convenient to take one pair of elements as phase reference for the array, e.g. $\phi_1 = 0$ in the former and $\phi_{N/2} = 0$ in the latter solution. Equation (11) will yield sufficiently accurate solutions for ϕ_r provided the distribution is reasonably smooth; this condition is satisfied in the cases to be described in which the nominal null-filling is limited to 50% ($m = 0{\cdot}5$). For constant null-filling, m may be placed outside the summation sign in Equation (11) so that the magnitude of the phase distribution (strictly sin ϕ_r) becomes proportional to m; it follows that for any given array, further cases of constant null-filling can be synthesized without repeating the above procedures.

---

* It is worth noting that Equations (9) and (11) are in the form of a transform pair.

Once the phase distribution ϕ_r has been evaluated using either Equation (9) or (11), the total current distribution may be written down directly as cos ϕ_r + j sin ϕ_r; the real part is the modified primary distribution and the imaginary part the quadrature null-filling distribution. In cases of practical interest, ($0{\cdot}25 \leqslant m \leqslant 0{\cdot}50$), the second-order errors, corresponding to the $\phi_r{}^2$ term in Equation (6), which are introduced by effectively null-filling a cos ϕ_r distribution as opposed to the original $1 + j0$ distribution, became significant. Methods for removing these errors are now described.

3.3. Non-oscillatory Solution

In this solution, all null-filling samples g_k are given the same sign so that the quadrature pattern does not cross the sin θ axis before reaching the half-power point (sin $\theta = 0{\cdot}5$ for $1{\cdot}0\lambda$ spacing). A continuous quadrature distribution $f(x)$ for a 20λ-array with $m = 0{\cdot}5$ has been synthesized using Equation (10) and is shown in Fig. 7. It will be observed that this typical distribution is very small in amplitude over most of its range but increases sharply towards the centre of the aperture. This fact is of some practical importance in the design of distributions for panel aerials. The radiation pattern of the resulting constant amplitude, variable phase, distribution formed by sampling the function $f(x)$ of Fig. 7 at $1{\cdot}0\lambda$ intervals has been computed and is plotted in Fig. 8. The error in the primary pattern manifests itself by alternately elevating and depressing the subsidiary lobes in the net pattern about their pre-null filled level.

Removal of these errors is surprisingly simple. The procedure is to impart a differential phase shift 2Δ to the resulting symmetrical distribution, i.e. to add $+\Delta$ radians to the top half and $-\Delta$ radians to the bottom half distribution. Without null-filling, a small differential phase shift would lead to a pattern:

$$p'(\sin\theta) \simeq p_0(\sin\theta) + 2\Delta\,\frac{\sin^2(\tfrac{1}{2}N\pi\sin\theta)}{\sin(\pi\sin\theta)} \tag{12}$$

where $p_0(\sin\theta)$ is given by Equation (5). It is shown in the Appendix, (Section 8), that in the presence of a quadrature distribution of the kind typified in Fig. 7, the second term in Equation (12) can cancel the error in the primary pattern (the $\phi_r{}^2$ term of Equation (6)) almost exactly. This is the cardinal step in the non-oscillatory solution; if the phase angle Δ is chosen carefully no iteration is

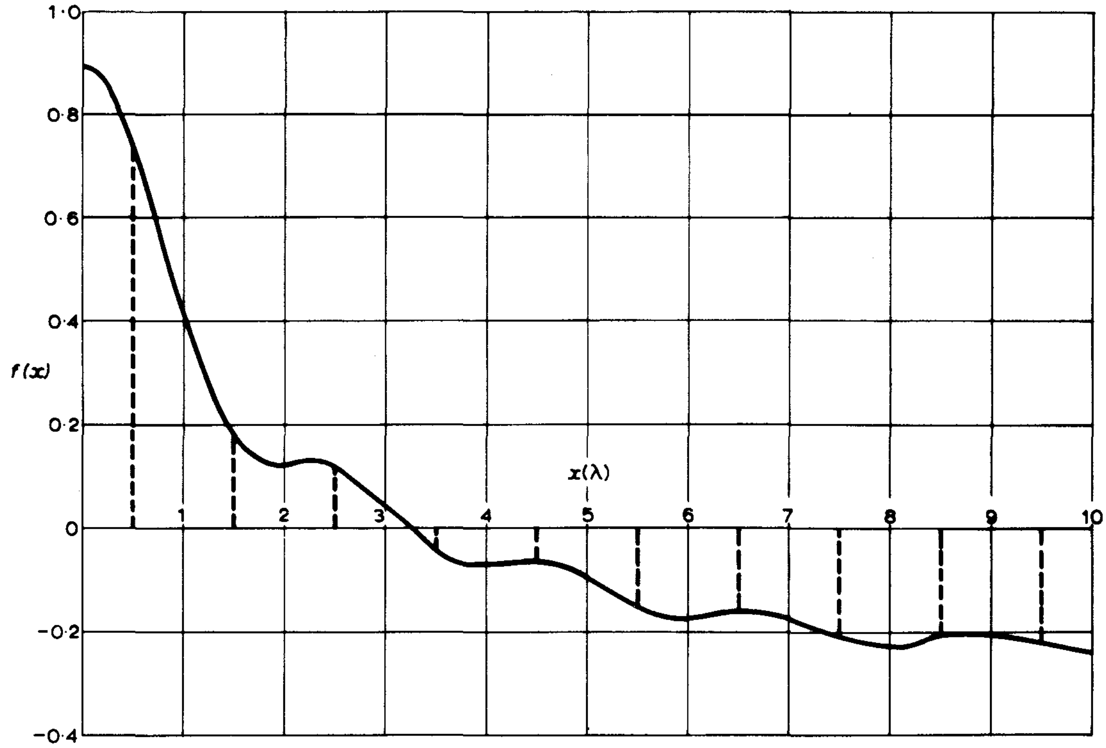

Fig. 7 - Synthesized continuous quadrature distribution for a 20λ-array with non-oscillatory null-filling,
$m = 0{\cdot}50$

------ direct samples for source quadrature currents, ϕ_r

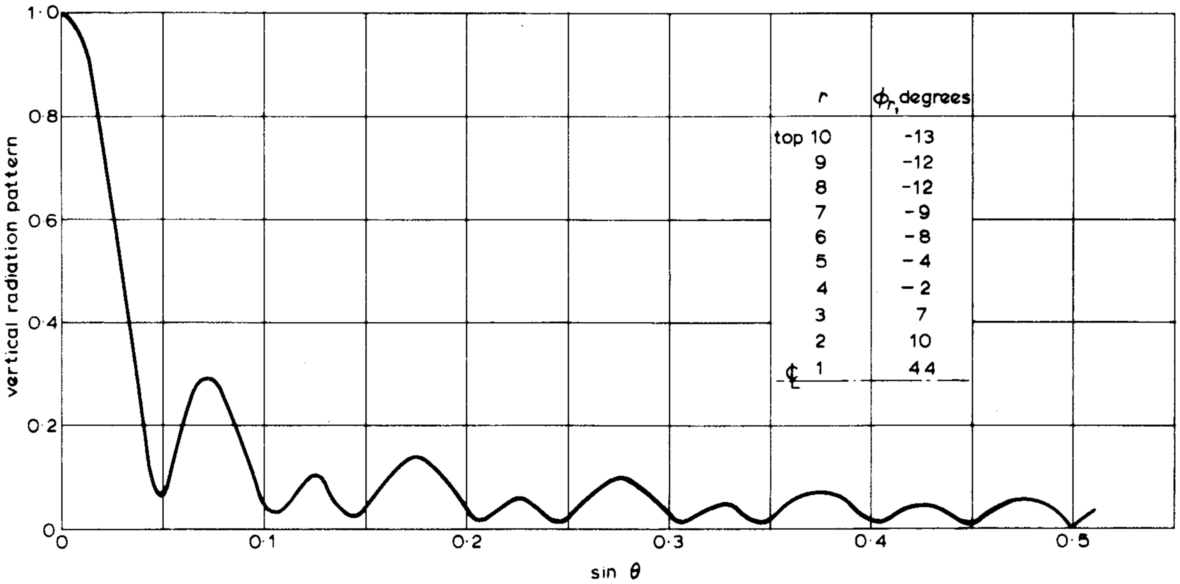

Fig. 8 - V.R.P. for a 20λ-array with uncorrected non-oscillatory null-filling, m = 0·50

required and a smooth approximation to the required cosecant pattern is obtained over the range $0 < \sin\theta \leqslant 0{\cdot}5$.

To demonstrate the process we refer to Fig. 9 in which are sketched the pertinent component radiation patterns for a 12λ-array. In this figure curves (*a*), (*b*) and (*c*) represent the first, second and third terms respectively of the right hand side of Equation (6). A small differential phase shift has little effect on these patterns; $p_0(\sin\theta)$ is scaled down by $\cos\Delta$ and the individual components of the primary error pattern (*c*), $-\phi_r^2\cos(\overline{2r-1}\pi\sin\theta)$, and the quadrature null-filling pattern (*b*), $j2\phi_r\cos(\overline{2r-1}\pi\sin\theta)$, are shifted on the $\sin\theta$ axis by $\Delta/(2r-1)\pi$ (Fig. 9 shows the resulting patterns (*b*) and (*c*) slightly displaced on the $\sin\theta$ axis). The primary error pattern (*c*) will be very nearly proportional to the single term $\cos(\pi\sin\theta)$ corresponding to the first pair of sources ($r = 1$), since these have the largest value of ϕ_r^2 whereas the null-filling pattern (*b*) approximates to $\operatorname{cosec}(\pi\sin\theta)$.*

Curve (*d*) in Fig. 9 represents the second term of the right hand side of Equation (12); this pattern component, which remains intact despite the introduction of the quadrature distribution, may be made to reduce the error pattern (*c*) considerably. Although curves (*c*) and (*d*) are different functions, (*d*) satisfies the requirements of being positive and real and of falling off with $\sin\theta$ at a convenient rate. As the two functions may be equated at a single point only, a compromise solution must be sought for the optimum reduction of the primary error pattern. Basing the solution on exact cancellation of the error by the mean of the differential phase pattern at $\sin\theta = 5/2N$ it may be shown (Appendix, Equation (33)) that Δ is given by the following semi-empirical relationship

$$\Delta \simeq \frac{\phi_1^2}{2}\sin(5\pi/N) \qquad (13)$$

where ϕ_1 is the relative phase of the innermost pair of elements, assuming $\phi_{N/2} = 0$. Although there is little justification for using Equation (13), it appears to work well in practice for uniform null-filling and large N. For non-uniform null-filling (m varying over range $0 < \sin\theta < 0{\cdot}5$) it is more accurate to use Equation (32) of the Appendix.

The final phase distribution Φ_r for the array is given by

$$\Phi_r = \phi_r \pm \Delta, \quad \begin{array}{l} r > 0, \text{ upper half of array} \\ r < 0, \text{ lower half of array} \end{array} \qquad (14)$$

where ϕ_r is given by Equation (9) or (11) and the upper sign applies to the upper half of the array. Applying Equation (13) to the null-filled 20λ-array of Fig. 8 we obtain $\Delta \simeq 0{\cdot}35$ radians and the computed radiation pattern corresponding to the revised phase distribution is shown in Fig. 10. In the second half of the pattern below the horizontal ($0{\cdot}5 < \sin\theta < 1{\cdot}0$), and the first half of the pattern above the horizontal ($-0{\cdot}5 < \sin\theta < 0$), the primary error pattern and the corrective pattern due to differential phase have identical polarities; their effects therefore add in these regions and lead to alternate large and small secondary maxima. There is some reduction of aerial gain due to the excessive levels of some of the secondary maxima, most of the reduction occurring in the first upper sidelobe.

---

* There is a formal relationship; since the primary error distribution is proportional to the quadrature power distribution, the corresponding error pattern is the autocorrelation function of the quadrature pattern.

It is evident that pattern correction with the non-oscillatory null-filling distribution produces a small incidental beam-tilt. This must be allowed for when choosing the linear phase progression required for the desired beam-tilt from Equation (8). A differential phase shift 2Δ is equivalent to a phase progression of $4\Delta/N$ radians per tier, providing Δ is small, so that this quantity must be subtracted from the right hand side of Equation (8) when evaluating ϕ_0, i.e.

$$\phi_0 = 2\left(\frac{\pi d\theta_0}{\lambda} - \frac{2\Delta}{N}\right) \text{ radians/tier} \qquad (15)$$

where θ_0, the desired beam-tilt angle, is small.

3.4. Oscillatory Solution

In this solution, the null-filling samples g_k alternate in polarity at successive null points whilst their amplitudes follow the cosecant specification, $mN/\pi k$, as before. The advantage of this method is that the quadrature pattern, over most of its range, crosses the sin θ axis near the points at which the primary pattern reaches its secondary maxima; the effect of this is that the secondary maxima of the net radiation pattern will have amplitudes which are little different from the corresponding amplitudes of the primary pattern.

A phase distribution for a 20λ-array with oscillatory null-filling to a nominal $m = 0{\cdot}5$ specification has been synthesized from Equation (9) by solving the 9×9 matrix equation. The distribution is shown in Fig. 11 and the resulting radiation pattern plotted in Fig. 12. Fig. 12 shows that such a radiation pattern will meet its specification over the restricted range $0 \leqslant \sin\theta \leqslant 0{\cdot}25$ (source spacing $1{\cdot}0\lambda$) but it will fail outside this range by a margin which increases as the half-period ($\sin\theta = 0{\cdot}50$) point of the pattern is approached.

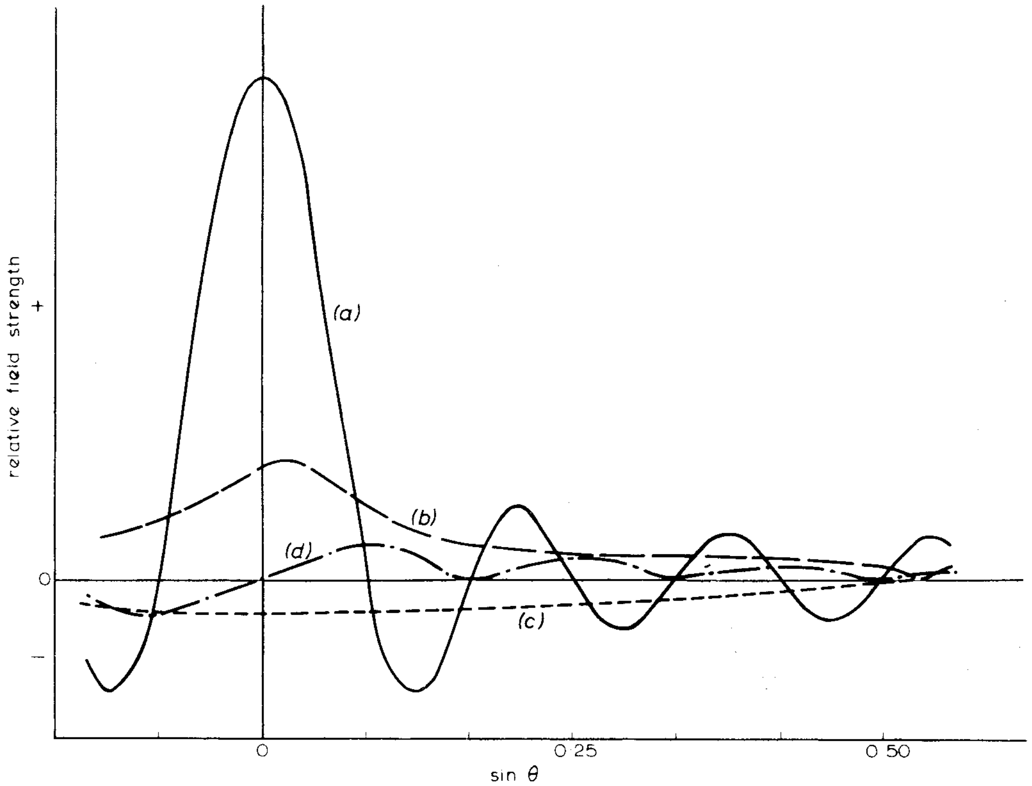

Fig. 9 - Mechanism of primary pattern error correction by differential phase shift between array-halves, non-oscillatory solution for a 12λ-array

(*a*) ———— primary pattern (*b*) — — — quadrature pattern

(*c*) - - - - - - - primary error pattern (*d*) —·—·— differential phase correction term

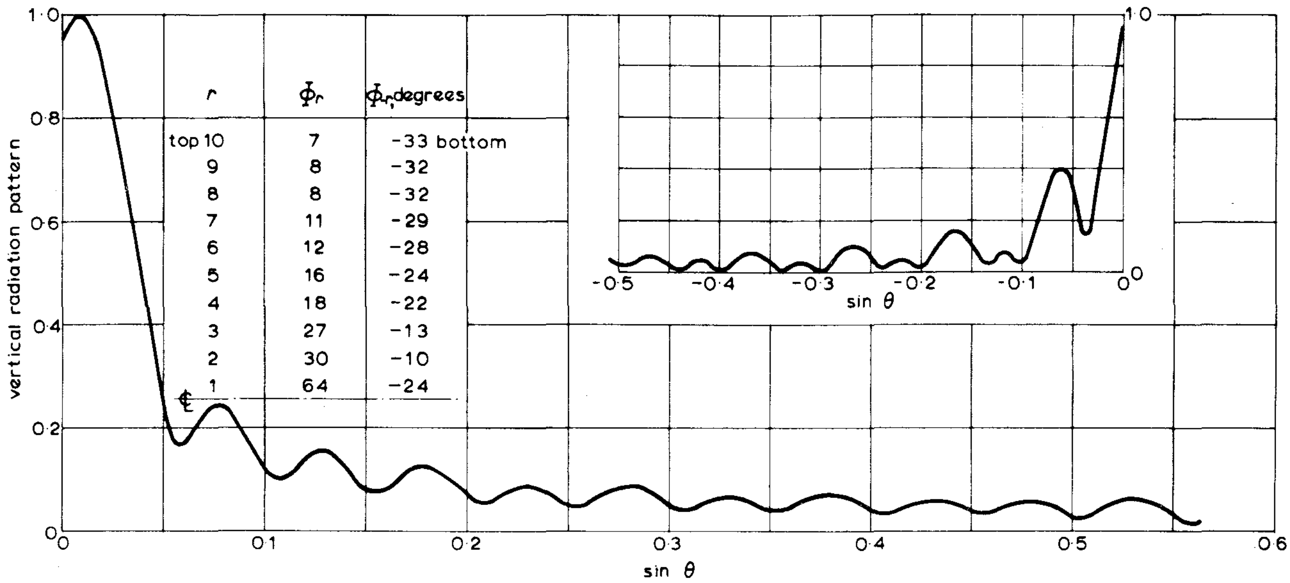

r	Φ_r	Φ_r, degrees
top 10	7	-33 bottom
9	8	-32
8	8	-32
7	11	-29
6	12	-28
5	16	-24
4	18	-22
3	27	-13
2	30	-10
1	64	-24

Fig. 10 - V.R.P. for a 20λ-array with non-oscillatory null-filling, m = 0·50 - differential phase correction of primary error pattern with Δ = 0·35 radians (20°)

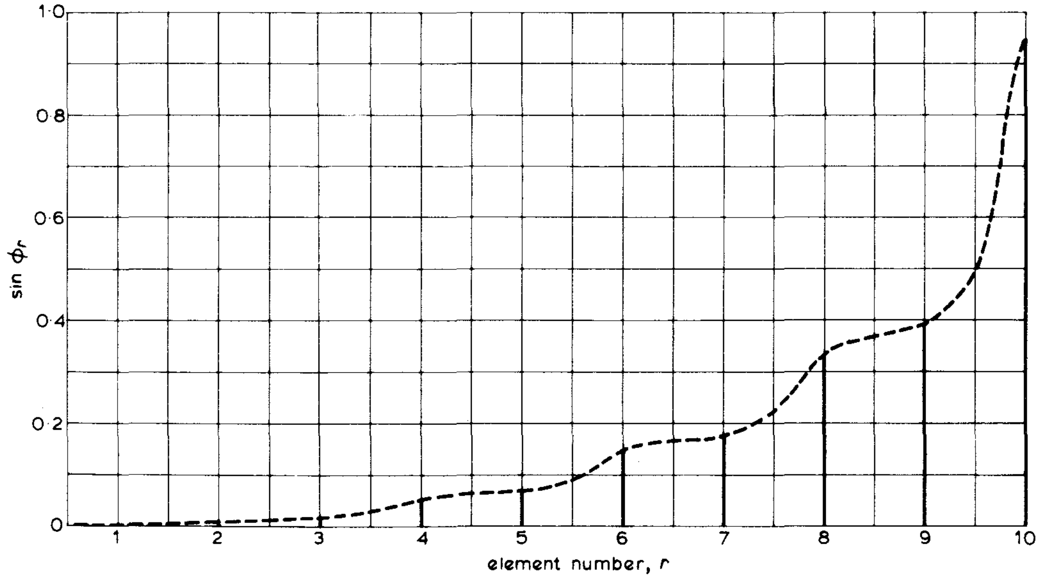

Fig. 11 - Synthesized discrete quadrature distribution for a 20λ-array with oscillatory null-filling, m = 0·50

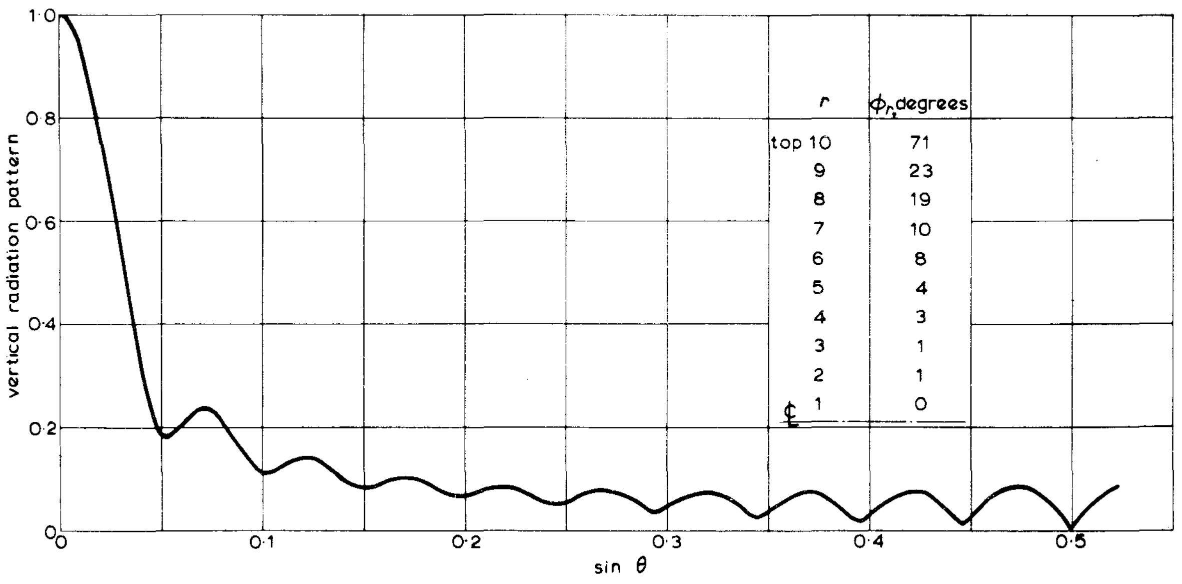

Fig. 12 - V.R.P. for a 20λ-array with uncorrected oscillatory null-filling, m = 0·50

The pattern fault with oscillatory null-filling resides mainly in the quadrature component which, because of the imposed symmetry, must fall to zero at the half-period point and which must therefore assume unnecessarily large amplitudes near this point in order to satisfy the null-filling specification. This is illustrated by Fig. 13 where curves (*a*), (*b*) and (*c*) represent the primary, oscillatory quadrature and primary error patterns respectively for a 12λ-array; the quadrature (null-filling) specification is shown by the vertical arrows.

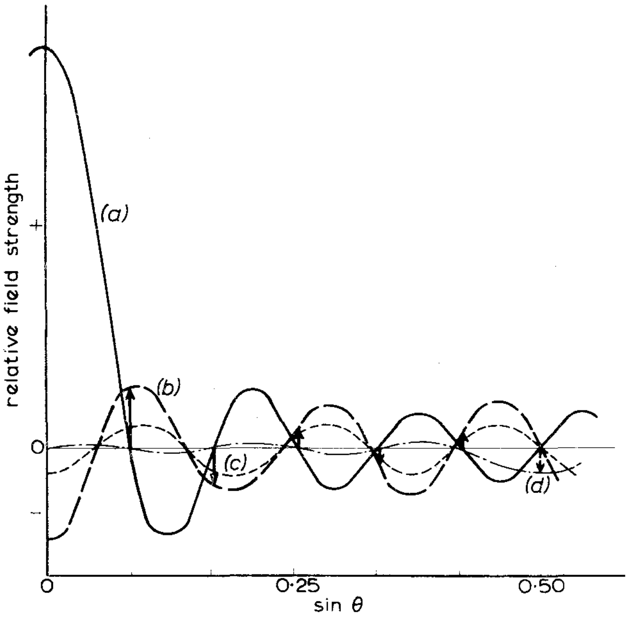

Fig. 13 - Mechanism of pattern error correction by oscillatory phase perturbation, oscillatory solution for a 12λ-array

(*a*)	———————	primary pattern
(*b*)	— — — —	quadrature pattern
(*c*)	– – – – – –	primary error pattern
(*d*)	—·—·—	oscillatory phase correction term

Correction of the pattern fault, as in the non-oscillatory solution, may be achieved by introducing some asymmetry into the phase distribution. In this case, however, we are dealing with a quadrature pattern error as opposed to a primary one. We look for a simple solution which (i) provides the desired degree of null-filling at sin θ = 0·5, (ii) reduces the side-lobe amplitudes near this point and (iii) leaves the prescribed null-filling amplitudes untouched. No ideal corrective solution has been found which does not require further iteration. A good solution would be to insert the sinc function K sinc(sin θ - 0·5) into the quadrature pattern. Curve (*d*) of Fig. 13 shows such a corrective pattern with the polarity of K made consistent with the sign alternation of the null-filling samples. This quadrature pattern may be approximately realized by supplementing the original null-filling quadrature distribution with a uniform quadrature distribution associated with a linear progressive phase shift of π radians per tier, i.e. a beam-tilt of $\sin^{-1}$ 0·5. At the array points, however, this distribution results in an odd amplitude perturbation which is in phase with the primary distribution so that it becomes impossible to maintain the constant amplitude condition without greatly modifying the quadrature distribution.

A reasonable compromise, however, is obtained by inserting the same sinc function K sinc (sin θ - 0·5) into the primary pattern in such a way as to augment the primary error pattern and further reduce the primary side-lobe level in the vicinity of sin θ = 0·5. The resulting odd amplitude perturbation is then in phase with the quadrature distribution so that the constant amplitude condition is easily maintained. The polarity of the sinc pattern correction term is now made the reverse of that shown in Fig. 13 and its amplitude at sin θ = 0·5

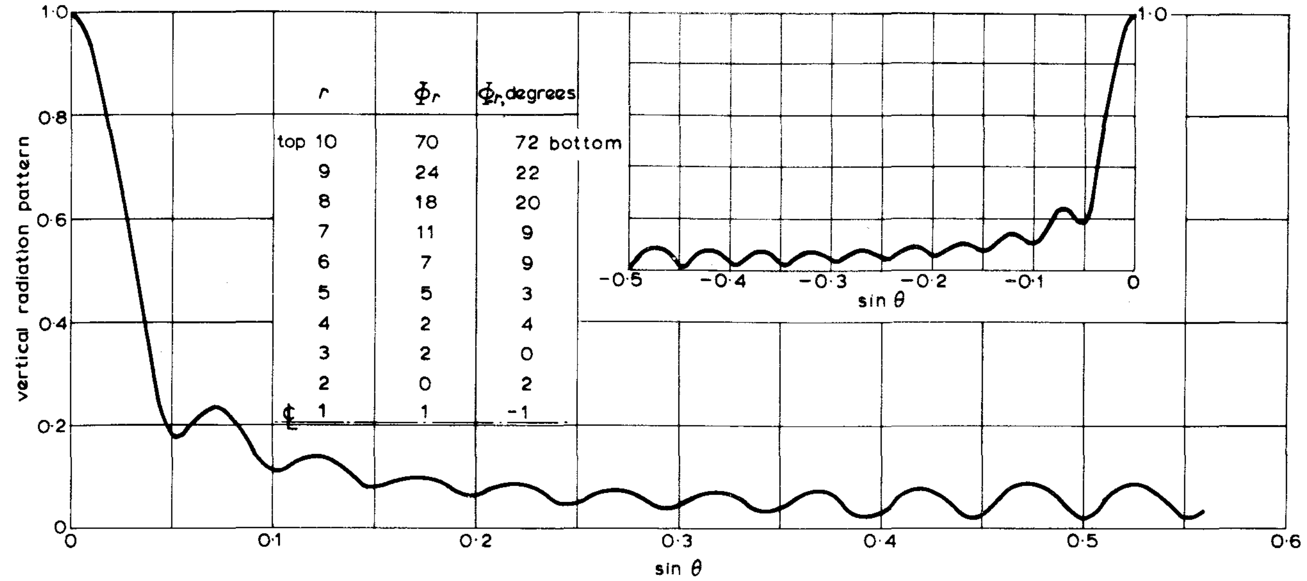

r	Φ_r	Φ_r, degrees
top 10	70	72 bottom
9	24	22
8	18	20
7	11	9
6	7	9
5	5	3
4	2	4
3	2	0
2	0	2
1	1	-1

Fig. 14 - V.R.P. for a 20λ-array with oscillatory null-filling, m = 0·50 - oscillatory phase correction of primary error pattern with δ = 0·016 radians (1·0°)

is determined by the specification $mN/\pi k$ with $k = N/2$, i.e. $K = 2m/\pi$. It follows that a uniform quadrature distribution of amplitude $2m/N\pi$ with a linear phase progression of π radians per tier (1·0λ spacing) will provide the desired pattern. Such a distribution results in an odd phase perturbation δ ($= \mp(-1)^r 2m/N\pi$) which is to be added to the previously obtained symmetrical distribution ϕ_r; the net phase distribution Φ_r is therefore given by

$$\Phi_r = \phi_r \mp (-1)^r \frac{2m}{N\pi}, \quad \begin{matrix} r > 0, \text{ upper half of array} \\ r < 0, \text{ lower half of array} \end{matrix} \qquad (16)$$

where the upper sign refers to the upper half of the array. The phase distribution for the 20λ-null-filled array whose pattern is shown in Fig. 12 has been revised according to Equation (16) with $m = 0·5$ and the resulting v.r.p. is shown in Fig. 14. In the second half of the pattern below the horizontal ($\sin \theta > 0·5$), the polarities of the primary error and the corrective patterns oppose each other and the side-lobe level is slightly increased in this region.

3.5. Relation Between Solutions

It has been shown in Sections 3.3 and 3.4 that there are two basic solutions available for meeting any given null-filling specification. There is in fact an analytical connection between the symmetrical (i.e. uncorrected) phase distributions derived from the oscillatory and the non-oscillatory quadrature patterns. The simple relationship is that the one distribution is the "inverse" of the other, i.e. if the two distributions are ϕ_r and ϕ'_t then,

$$\phi_r = \phi'_{\frac{N}{2}+1-r} \qquad (17)$$

Equation (17) shows that, having synthesized the quadrature pattern corresponding to one solution, the other may be written down directly, if required, without further synthesis. The subsequent corrective procedures are of course different. The relationship is illustrated diagrammatically in Fig. 15.

The result given in Equation (17) may be demonstrated by starting from Equation (9) as follows: Let g_k and g'_k be the null-filling specifications corresponding to the phase distributions ϕ_r and ϕ'_t respectively, i.e. $g'_k = (-1)^k g_k$. Then we may write

$$g_k = 2\sum_{r=1}^{N/2} \phi_r \cos(\overline{2r-1}\,\pi k/N)$$

and similarly for g'_k with t and ϕ'_t replacing r and ϕ_r respectively in this expression. Inserting $t = N/2 + 1 - r$ into the relation for g'_k and manipulating we have

$$g'_k = 2\cos \pi k \sum_{r=N/2}^{1} \phi'_{\frac{N}{2}+1-r} \cos(\overline{2r-1}\,\pi k/N)$$

since k is an integer. If g_k and g'_k represent the oscillatory and the non-oscillatory null-filling samples we know that $g'_k = (-1)^k g_k$. It follows, therefore, that $\phi_r = \phi'_{N/2+1-r}$ which is the required relation.

Finally, it is worth noting that we may choose either polarity for the uncorrected quadrature patterns; the polarities correspond to leading or lagging phase distributions. There may be some practical advantage in maintaining either a positive or a negative phase-slope over some part of the array.

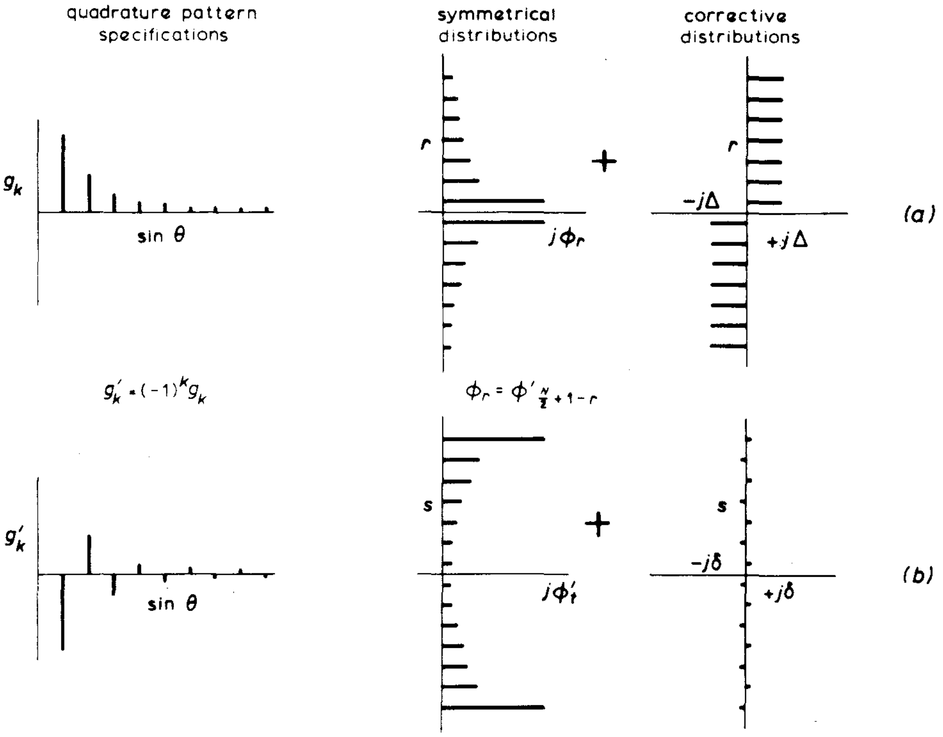

Fig. 15 - Diagrammatic illustration of the relation between solutions and their correction
(*a*) non-oscillatory solution (*b*) oscillatory solution

4. APPLICATION TO U.H.F. TRANSMITTING AERIALS

Although the synthesis techniques described in Section 3 are for point source arrays they may be readily applied to practical u.h.f. transmitting aerials. The synthesis is performed by noting that the radiation pattern of a multi-tiered aerial of similar elements is given by multiplying the pattern of the equivalent point source array by the pattern of one element. The tiers may comprise simple vertical dipoles (BBC u.h.f. relay-station aerials) or alternatively, simple horizontal dipoles grouped into identical "panels" (BBC u.h.f. main-station aerials). Each type will be treated in turn and some consideration will also be given to the question of aerial impedance, gain reduction and pattern bandwidth.

4.1. Aerials with Individually-fed Tiers

A practical arrangement for a low-power (relay) aerial is shown in Fig. 16. The aerial consists of vertical dipoles spaced 1·0λ; it is split into halves, each half being branch fed from an $N/2$: 1 power splitting transformer. The cable lengths l_r are cut according to the synthesized phase distribution Φ_r and, with the transformers placed below the aerial, the mean cable length must be made at least $N\lambda$. The diplexer is at ground level so that with a 45 m (150 ft) tower, the main feeder lengths are around 52 m (170 ft); this means that at 500 MHz using conventional cables, the diplexer and transformers will be about 100λ apart.

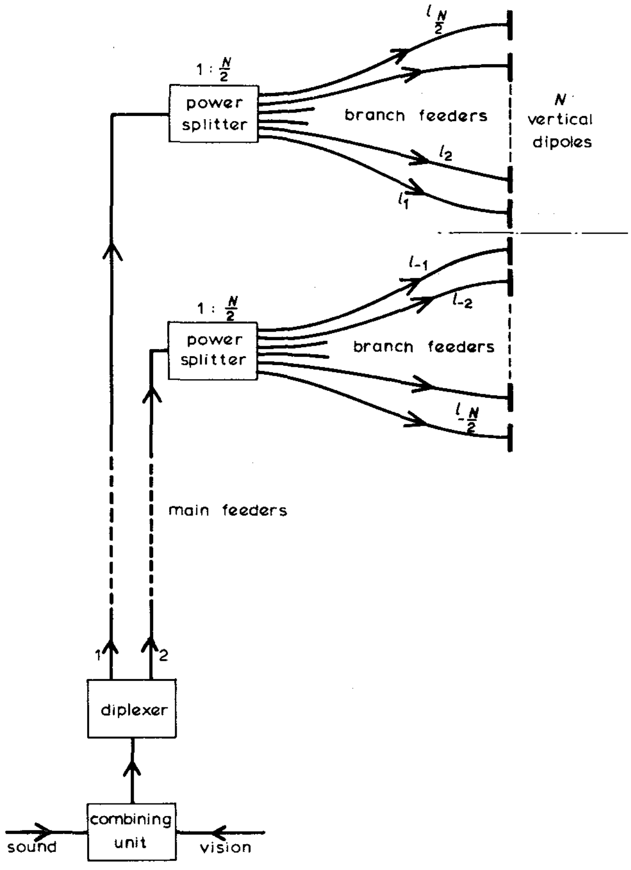

Fig. 16 - General arrangement of low power u.h.f. aerial

If such an aerial were uniformly fed, its v.r.p. would be given by $f(\theta)p_0(\sin\theta)$ where $f(\theta)$ is the v.r.p. of a single tier and $p_0(\sin\theta)$ is given by Equation (5). It therefore follows that the point-source synthesis procedure may be applied provided the null-filling amplitudes g_k are inversely weighted by the factor $f(\theta)$. For half-wave dipoles, we set

$$g_k = \frac{m\cot\theta}{\cos(\frac{\pi}{2}\sin\theta)} \qquad (18)$$

and then use either Equation (9) or (11) for synthesis. In a typical 16-tier aerial, the null-filling was specified as $m = 0{\cdot}50$ for $0 < \theta < \pi/12$ and $m = 0{\cdot}25$ for $\pi/12 < \theta < \pi/6$. Equation (11) was used to synthesize a non-oscillatory quadrature pattern which satisfies this specification; the differential phase correction 2Δ was derived from Equation (32) and found to be approximately 36°. This figure was increased to 50°, with negligible deterioration of the v.r.p., in order to reduce the aerial mismatch (the mechanism of this reduction will be clarified in Section 4.3). The beam-tilt was required to be 1·75° so that an additional progressive phase shift of 5° per tier (Equation (15)) was superposed on the phase distribution.

The centre-frequency v.r.p. for the 16-tier aerial is shown in Fig. 17 together with the null-filling specification for the pattern. It is seen that there is some latitude at the pattern minima; this allows the specification to be satisfied over a band of frequencies and also gives the pattern some resistance to the effects of phase errors.

A split aerial system (Fig. 16) may introduce a differential phase error (d.p.e.) between array halves either through cutting inaccuracies of the main feeders or through differential thermal expansion between them. With 100λ feeders, a 10° d.p.e. (i.e. a uniform phase error of 5° over the upper half and -5° over the lower half aerial) corresponds to an error in length of 0·028%; this is equivalent to a feeder length difference of 14 mm (0·54 in.) at 500 MHz or a temperature difference of approximately 20°C between feeders. Computation has shown that the v.r.p. of Fig. 17 remains within specification for d.p.e.s up to a maximum of ±10°. The actual effects on the radiation pattern shape may be seen, in very much magnified form, by comparing Fig. 8 with Fig. 10; the former shows the null-filled v.r.p. of a 20λ-array with an effective d.p.e. of -40°.

The effects of random phase errors will be discussed in Section 5.2.

4.2. Panel Aerials

At high-power u.h.f. stations the aerial apertures are large (20λ to 40λ) and, with horizontal polarization, the inter-tier spacing may be reduced to around 0·5λ. It is then more practicable, with such a large number of elements, to build up the required aerial aperture from standard vertical groups or panels of horizontal dipoles. A typical panel would be 2·0λ long and carry four elements spaced 0·5λ apart and 0·25λ away from a reflecting screen, at the design frequency. Stacks of panels

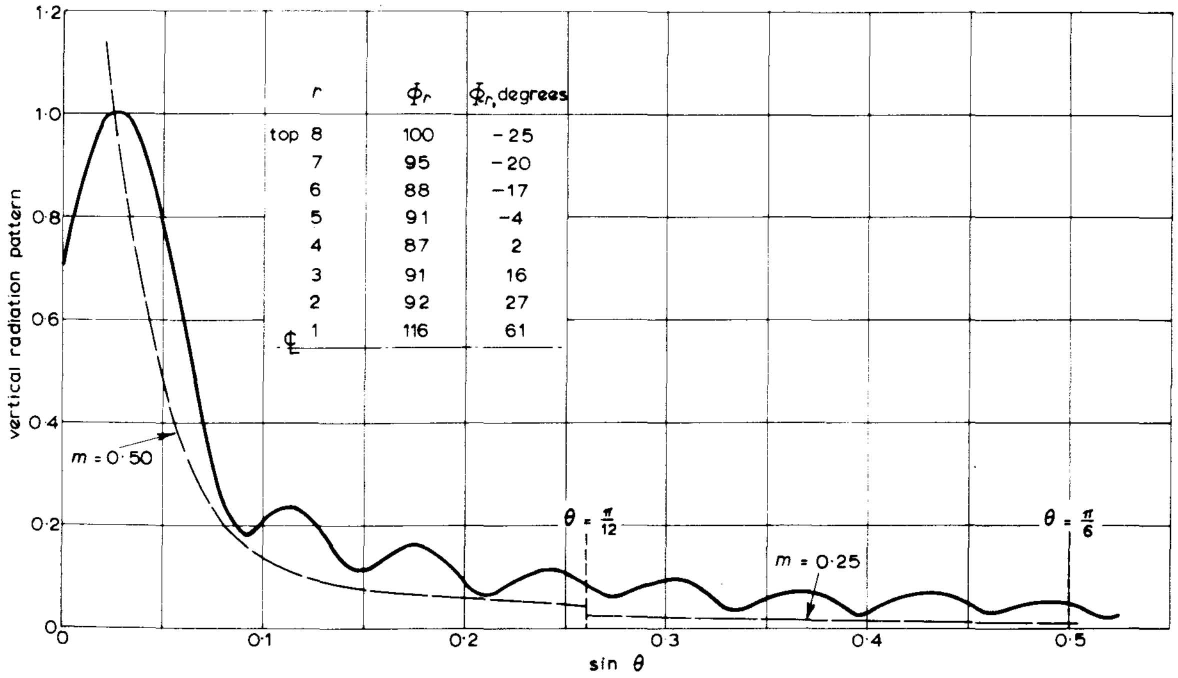

r	ϕ_r	Φ_r, degrees
top 8	100	-25
7	95	-20
6	88	-17
5	91	-4
4	87	2
3	91	16
2	92	27
1	116	61

Fig. 17 - V.R.P. for a 16-tier relay aerial with vertical half-wave dipoles spaced 1·0λ apart - non-oscillatory null-filling with $\Delta = 0{\cdot}44$ radians (25°)

———— null-filling specification, $m = 0{\cdot}50$ and $0{\cdot}25$

are mounted on the mast faces and are divided into two equal vertical sections for operational reasons; impedance considerations would normally lead to a progressive phase shift of 90° per stack around the mast. Here, we concern ourselves with the problem of null-filling the v.r.p. of a single stack of panels; the synthesized phase distributions must be such that the panel phase distributions are identical for the entire stack.

Let us consider a stack of M (even) panels, each panel comprising n (even) horizontal dipoles spaced s wavelengths apart and q wavelengths from a perfectly-conducting screen. If the Mn elements of the stack are energized with uniform co-phased currents, the v.r.p. is given by,

$$p(\theta) = \frac{\sin(Mn\pi s \sin\theta)}{\sin(\pi s \sin\theta)} \sin(2\pi q \cos\theta) \qquad (19)$$

where the first factor is the v.r.p. of the uniform array and the second factor is due to the presence of the screen. We recall from array theory that the array factor in Equation (19) may be split into more elementary components. For example, we may write,

$$p(\theta) = \frac{\sin(M\pi ns \sin\theta)}{\sin(\pi ns \sin\theta)} \times \frac{\sin(n\pi s \sin\theta)}{\sin(\pi s \sin\theta)}$$

$$\times \sin(2\pi q \cos\theta) \qquad (20)$$

in which the first factor is the v.r.p. of the "coarse" array of M sources placed at the mid-points of the panels, i.e. spaced ns wavelengths apart, and the second factor is the v.r.p. of the panel itself (without the reflecting screen).

Alternatively, we may write,

$$p(\theta) = \frac{\sin(2M\pi\frac{ns}{2} \sin\theta)}{\sin(\pi\frac{ns}{2} \sin\theta)} \times \frac{\sin(\frac{n}{2}\pi s \sin\theta)}{\sin(\pi s \sin\theta)}$$

$$\times \sin(2\pi q \cos\theta) \qquad (21)$$

in which the first factor is the v.r.p. of an array of $2M$ sources placed at the mid-points of each half-panel, i.e. spaced $ns/2$ wavelengths apart, and the second factor is the v.r.p. of the half-panel itself. Equations (20) and (21) lead to two simple solutions for null-filling the v.r.p. of a panel aerial using the techniques described in Section 3; in both cases, the null-filling specification is inversely weighted by the screen factor $\sin(2\pi q \cos\theta)$ prior to synthesis. In essence, two procedures for null-filling panel aerials are as follows:

(i) Multiplicative method

The v.r.p.s of the coarse array and of the panel (both given in Equation (20)) are null-filled separately and to such a degree that the product of the patterns at the original null-points satisfies the overall null-filling specification. It will be shown that the array null-filling must employ the oscillatory solution for synthesis (Section 3.4) since we require a symmetrical pattern from this factor; also, that the two v.r.p.s may be null-filled independently.

or

(ii) Panel-tilt method

The v.r.p. of an array of $2M$ sources spaced $ns/2$ wavelengths apart (Equation (21)) is null-filled using either the oscillatory or the non-oscillatory solutions for synthesis (Sections 3.3, 3.4). The cosecant specification employed should be inversely weighted by the v.r.p. of a half-panel i.e. $n/2$ sources spaced s wavelengths apart. The resulting phase distribution is then examined for linearity; those panels over which the phase-slope is large are tilted physically so that the fine distribution is followed more accurately whereas the remainder are just given the mean phase over their lengths.

These procedures will now be examined in greater detail. By way of example we shall consider a stack of 10 panels, with 4 dipoles per panel mounted 0·5λ apart and 0·25λ from the panel screen, i.e. $M = 10$, $n = 4$, $s = 0{\cdot}5$, and $q = 0{\cdot}25$.

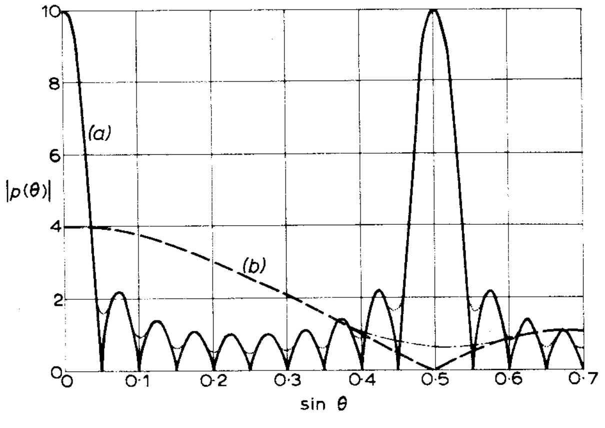

Fig. 18 - Multiplicative method for null-filling the v.r.p.s of panel aerials

——— (a) v.r.p. of 10-source array with 2·0λ spacing

– – – (b) v.r.p. of panel with 4 elements spaced 0·5λ apart

……… null-filling in (a) —·—·— null-filling in (b)

In the multiplicative method we commence by null-filling the array v.r.p., $\sin(20\pi \sin\theta)/\sin(2\pi \sin\theta)$ shown in Fig. 18. This pattern repeats every 0·5 in $\sin\theta$, is symmetrical about $\sin\theta = 0{\cdot}25$ and has nulls every 0·05 in $\sin\theta$ (except at the positions of the major lobes). The array pattern repeats at the null-frequency of the panel v.r.p., $\sin(2\pi \sin\theta)/\sin(0{\cdot}5\pi \sin\theta)$, so that its nulls can be filled independently of those of the panels. In Fig. 18 we show the two patterns and indicate the form of null-filling to be employed. The array v.r.p. must be null-filled symmetrically about its maxima and to the same degree (m-value) as that required in the final pattern. This ensures uniform null-filling because the envelope of the original array v.r.p. becomes the full cosecant pattern on multiplication by the original panel v.r.p. Because of this symmetry requirement, we must use the oscillatory solution for the synthesis of the array distribution (Section 3.4). Either solution may be employed for the panel. In the present case we have used Equation (9) for synthesizing the array distribution for $m = 0{\cdot}5$ by setting $N = 20$ and selecting even values of r; this gives a symmetrical phase distribution for the panels of 47°, 11°, 8°, 1°, 0° to which is added an odd phase perturbation ±2° (Equation (16)) in order to fill the null at $\sin\theta = 0{\cdot}25$. At $\sin\theta = 0{\cdot}5$ we require a null-filling amplitude of $2/\pi$ so that this null of the panel v.r.p. must be filled to an amplitude of $1/5\pi$; this may be accomplished by advancing (or retarding) the phase of the outermost pair of dipoles on each panel by approximately 5°. The computed v.r.p. for the complete distribution is shown in Fig. 19 together with the cosecant pattern specification. Beam-tilt has been omitted; the required tilt may be achieved by superposing separate uniform progressive phase shifts on the two component phase distributions. It will be seen that the v.r.p. is only just acceptable over the range $0{\cdot}2 < \sin\theta < 0{\cdot}3$; this is due to partial failure of the corrected oscillatory solution used for synthesizing the array distribution (see, for example, the region near $\sin\theta = 0{\cdot}5$ in Fig. 14). The elevation of the v.r.p. near $\sin\theta = 0{\cdot}5$ occurs because the null-filling of the panel v.r.p. has spread beyond the major lobe of the array pattern, as demonstrated in Fig. 18.

In the panel-tilt method we commence by null-filling an array of 20 sources with 1·0λ spacing i.e. the v.r.p. $\sin(20\pi \sin\theta)/\sin(\pi \sin\theta)$. Either solution may be employed (Sections 3.3, 3.4) but here we must weight the null-filling amplitudes with the inverse of the half-panel pattern, $\sin(0{\cdot}5\pi \sin\theta)/\sin(\pi \sin\theta)$, i.e. $2\sec(0{\cdot}5\pi \sin\theta)$. Choosing the non-oscillatory solution we arrive at a symmetrical phase distribution of 0°, 1°, 1°, 4°, 5°, 9°, 11°, 19°, 24°, 62° with a differential phase correction of 40°. In this distribution we have specified two phases per panel i.e. (0°, 1°) and (1°, 4°) etc. The panels, however, are to be electrically co-phased over their lengths; the required phase-slope is then obtained from a suitable differential stagger of the panel elements. This combination of panel-phasing and panel-tilt provides the required phase distribution accurately over a large range of inclination angles θ. Suppose for example, we horizontally stagger a single source x_r wavelengths away from the vertical line containing the phase reference point for its array. This is equivalent to an electrical phase ϕ_r' given by

$$\phi_r' = 2\pi x_r \cos\theta \tag{22}$$

which is θ dependent. If x_r is chosen to provide ϕ_r exactly at $\theta = 0{\cdot}37$ radians (21°), then the effective phase distribution ϕ_r' will be accurate to within 7% of that specified over the range $0 < \sin\theta < 0{\cdot}5$. A 2λ-panel requiring a distribution ϕ_i, ϕ_j should therefore be fed with co-phased currents of phase $(\phi_i + \phi_j)/2$ and be given a differential stagger $\pm 1{\cdot}07(\phi_i - \phi_j)/4\pi$ wavelengths i.e. a tilt of $\pm\sin^{-1}\{0{\cdot}17(\phi_i - \phi_j)\}$. With this distribution, the phase-slope over the panels is small except for the central pair with phases (44°, 82°) and (42°, 4°). The computed v.r.p. for the distribution, with only

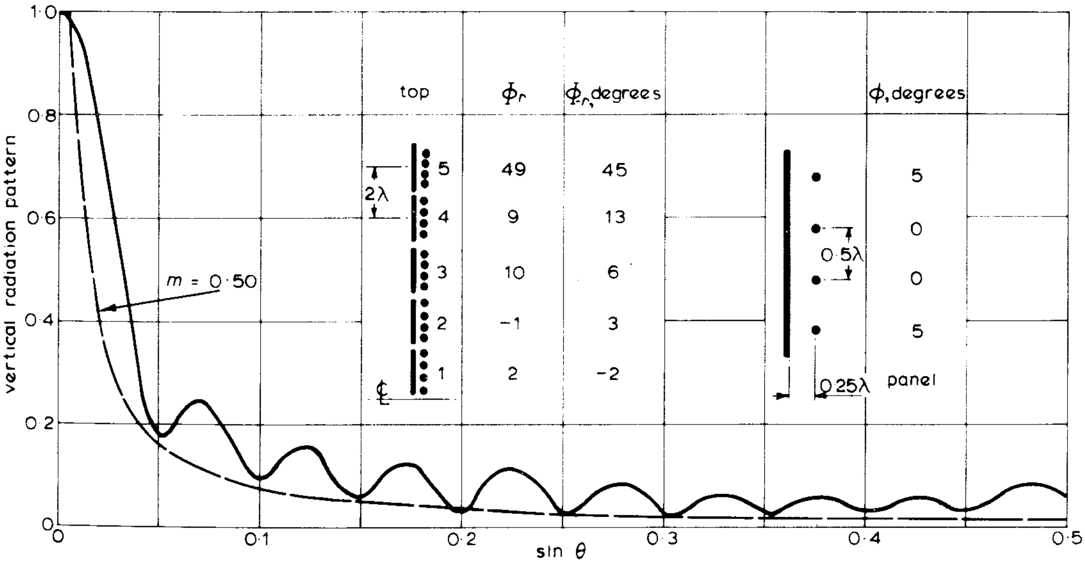

Fig. 19 - V.R.P. for a 10-panel aerial with 4 horizontal dipoles/panel spaced 0·5λ apart - multiplicative null-filling

——— ——— ——— ——— null-filling specification, $m = 0{\cdot}50$

the central panels tilted (6·5°) is shown in Fig. 20 together with the null-filling specification; also shown is the corresponding v.r.p. (dotted curve) with all the panels tilted appropriately. It is seen that the v.r.p. with the central panels tilted is quite satisfactory and differs very little from that derived from the full distribution.

If we employ the oscillatory solution instead, the symmetrical distribution is inverted (Section 3.5); the addition of a uniform progressive phase shift of 4°/wavelength to maintain a beam-tilt of 0·5° results in a final distribution (commencing with the top panel) of:

(100°,58°), (49°,37°), (31°,23°), (18°,11°), (7°,2°), (-2°,-5°), (-9°,-10°), (-13°,-13°), (-15°,-11°), (-10°,-24°)

In this case we may adequately realise the distribution by tilting only the outermost pair of panels. The progressive phase shift introduced for beam-tilt, however, has reduced the phase-slope of the bottom panel to one-third of that of the top panel. In fact if the panel-tilt is restricted solely to the top panel (downwards), it may be shown that the resulting v.r.p. is still perfectly satisfactory. Alternatively, if a lagging symmetrical distribution is used for the oscillatory solution, the final distribution is the negative inverse of that given above, i.e. (24°,10°), (11°,15°), ... (-58°,-100°). We can now restrict panel-tilt to the bottom panel only and in this case the downward tilt points the panel away from the main array; this may have some advantage if mutual impedance effects make the actual realization of the distribution difficult to achieve (Section 5.1).

Finally we note that with suitable shifting of the electrical phase of a panel, its axis of tilt can be moved from the centre to its end-point and this may be practically advantageous; the change in v.r.p. will be negligible.

4.3. Impedance, Gain Reduction and Bandwidth

In this section we consider the impedance, gain reduction and bandwidth of arrays null-filled by phase perturbation; first we discuss impedance.

A split aerial system (see, for example, Fig. 16) employs a diplexer to divide the transmitter power equally between the two aerial-halves whilst at the same time providing isolation between them. Suppose, for example, we employ a 90°-diplexer[10]. Waves emanating from the two output ports of this type of diplexer have a phase displacement of $\pi/2$ radians which must be taken into account when deducing the branch feeder distribution l_r from the synthesized phase distribution Φ_r. Suppose such a diplexer (Fig. 21) is terminated at ports 2 and 4 with reflexion coefficients ρ_2 and ρ_4. Then if port 3 is matched, the input reflexion coefficients ρ_{in} at port 1 (transmitter) is given by $\frac{1}{2}(\rho_4 - \rho_2)$. The output waves from ports 2 and 4 are in phase quadrature so that the aerial-halves must be fed inversely in quadrature to preserve the phase distribution Φ_r at the aerial. If, therefore, ρ_2 and ρ_4 represent the net

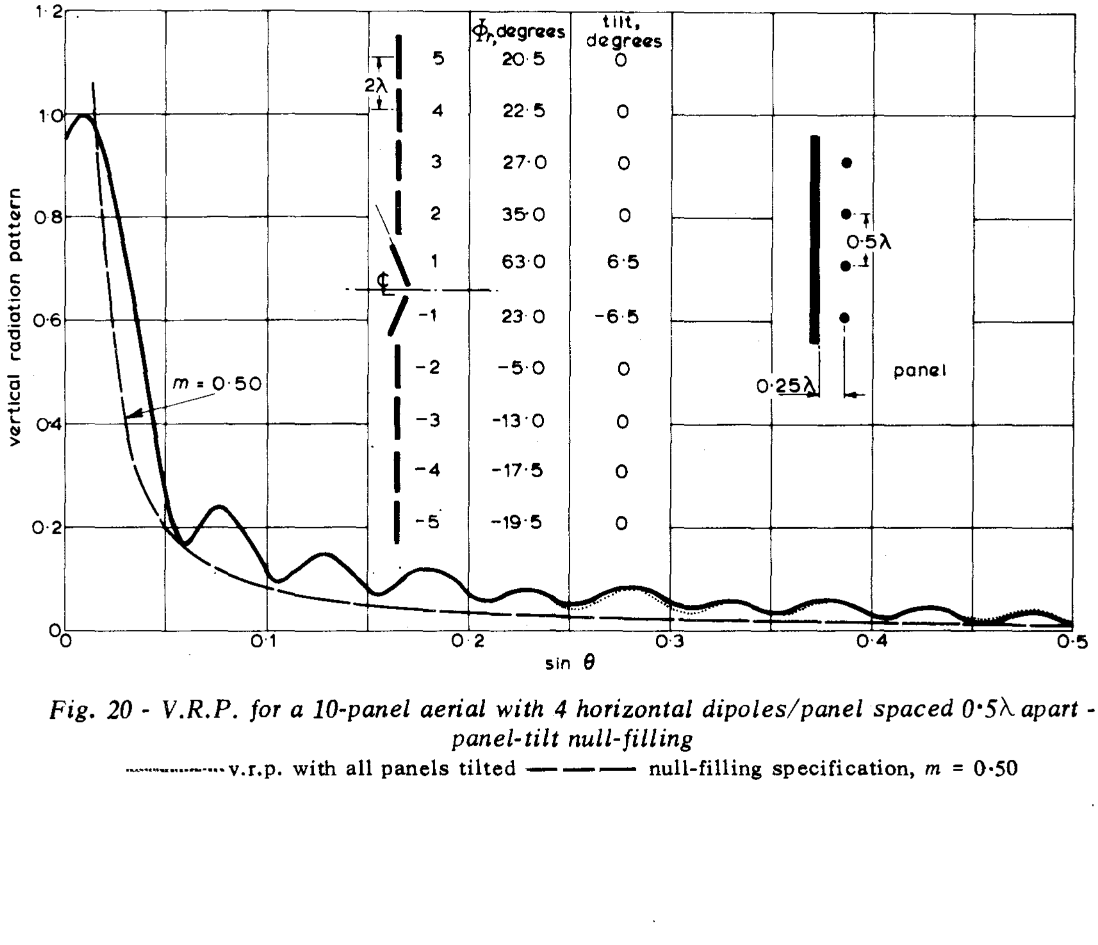

Fig. 20 - V.R.P. for a 10-panel aerial with 4 horizontal dipoles/panel spaced 0·5λ apart - panel-tilt null-filling

.................v.r.p. with all panels tilted ——— null-filling specification, m = 0·50 reflexion coefficients of the upper and lower halves of the aerial, we may write

$$|\rho_{in}| = \frac{|\rho|}{N} \left| \sum_{r=-\frac{N}{2}}^{N/2} \varepsilon^{j2\Phi_r} \right| \qquad (23)$$

in which $|\rho|$ is the reflexion coefficient of the branch feeder terminations (dipoles), assumed equal, and Φ_r is the synthesized phase distribution for the array. In this expression, we have ignored inter-tier mutual impedance and mismatch in the branch feeder power splitting transformers. Nevertheless, Equation (23) was found to be reasonably accurate in the design of a typical relay aerial and should be particularly useful for determining the upper limit for the dipole reflexion coefficient $|\rho|$ which will just satisfy the specification for total aerial matching $|\rho_{in}|$ with a given degree of null-filling. A symmetrical phase distribution combined with a differential phase shift of $\pi/2$ radians between aerial halves would make $\rho_{in} = 0$. It will be seen that the degree of aerial mismatch largely depends upon the corrective and beam-tilting distributions which in turn depend upon the type of solution employed for synthesis. For example, if we consider the 16λ-aerial of Section 4.1 and use the non-oscillatory solution for synthesis (distribution and v.r.p. given in Fig. 17) we find that $|\rho_{in}| = 0{\cdot}17\,|\rho|$; if, on the other hand, the oscillatory solution is employed, the aerial mismatch is increased to $|\rho_{in}| = 0{\cdot}29\,|\rho|$. A typical value for $|\rho|$ is 10%.

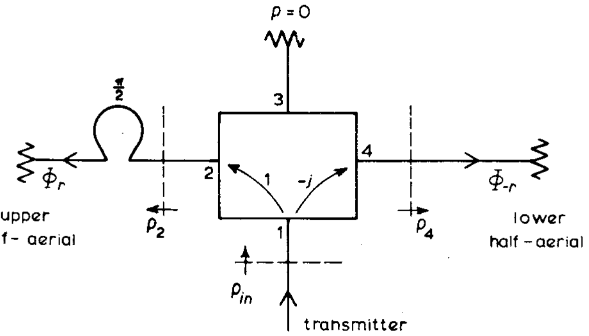

Fig. 21 - Terminated 4-port 90°-diplexer

Finally, it is important to note that any transmitter mismatch will cause reflected waves to return to the radiating elements of the aerial; the phase distribution of the first delayed signal (resulting from two reflexions) is approximately $-3\Phi_r$ for one half-aerial (top half, Fig. 20) and $3\Phi_r$ for the other. If the main lobe of the "reflected v.r.p." falls outside the main lobe of the main pattern, the delayed signal level will be greatly enhanced and such a contingency should be taken into account in drawing up the aerial impedance specification.

The process of null-filling inevitably reduces the gain of a multi-tiered aerial.

An array of N isotropic sources carrying equal co-phased currents of unit amplitude will produce a main lobe amplitude $\hat{E}$ given by $\hat{E} \simeq N$. If the phase of each source is perturbed by Φ_r, the resulting amplitude $\hat{E}'$ may be expressed as

$$\left(\frac{\hat{E}'}{\hat{E}}\right)^2 = \frac{(\sum_r \cos \Phi_r)^2 + (\sum_r \sin \Phi_r)^2}{N^2} \qquad (24)$$

If N is large the phase perturbations have negligible effect on the total power radiated, even if the mutual impedances between adjacent tiers are high. Equation (24) may therefore be used to determine the gain reduction g (dB) of an array which has been null-filled by phase perturbation provided the phase distribution Φ_r substituted in it is first modified to reset the beam-tilt to zero; there will be little error in using the symmetrical (i.e. uncorrected) distribution ϕ_r for both synthesis solutions. If we then make the further approximation that the phase departures of all ϕ_r from their mean, $\bar{\phi}$, are small we can show that,

$$g \simeq 10 \log_{10}\{1 - \frac{2}{N}\sum_{r=1}^{N/2}(\phi_r - \bar{\phi})^2\} \qquad (25)$$

Furthermore, the quantity inside the brackets is simply $1 - \sigma^2$ where σ is the standard deviation of the phase distribution ϕ_r in radians and is also small. We may therefore replace the logarithmic expression with its first order approximation and write finally,

$$g \simeq -4{\cdot}34\sigma^2, \text{ dB} \qquad (26)$$

A 20λ-array with 50% null-filling (Figs. 10 and 14) has a gain reduction given by Equation (26) of 0·4 dB, which is in very good agreement with the figures obtained from Equation (24) and also from pattern integration. Since the magnitude of ϕ_r is proportional to m for a given array, we can see from Equation (26) that g is proportional to m^2; for example, with the same 20λ-array, 25% null-filling yields a gain reduction of 0·1 dB.

In practice, the null-filled v.r.p.s must remain within specification over a finite frequency bandwidth. The bandwidth associated with a prescribed distribution is best explored by pattern computation since a variation in frequency changes many interrelated factors and no simple expression for bandwidth is available. The first-order effects of frequency variation are easily estimated however. A fractional frequency variation $\pm f$ changes the phase distribution ϕ_r by the same fraction so that, from Equation (9), the amplitudes of the v.r.p. at the null-points, g_k, also change by $\pm f$. In addition, the null-spacing is varied by $\pm f$ and beam tilt is unaffected. Computation has shown that the non-oscillatory synthesis solution yields a ±10% bandwidth per se because the null-filling specification is more than satisfied at the design (i.e. centre) frequency. With the oscillatory solution, the centre frequency distribution g_k should be increased by 10% prior to synthesis so that the resultant v.r.p. may satisfy the null-filling specification at the lower end of the frequency band.

5. MISCELLANEOUS CONSIDERATIONS

The phase distributions described in the previous sections are realized by energizing the aerial elements (dipoles or panels) from a common drive-point via branch feeders cut in length according to the prescribed phases. In general, the actual current distributions will be in error because of inter-tier mutual coupling and errors in the electrical lengths of the feeders. Errors due to mutual coupling are calculable and can be allowed for; the effects of random errors in feeder length are best treated statistically. Detailed treatment is outside the scope of this report so these points are only briefly discussed.

5.1. The Effects of Inter-tier Mutual Coupling

In most practical arrangements of branch-fed, multi-tier aerials, particularly those with closely spaced parallel dipoles, the effects of mutual coupling cannot be ignored. In such cases, the actual current distribution will exhibit both phase and amplitude errors if we attempt to realize a synthesized phase distribution Φ_r by cutting feeders exactly to a distribution l_r given by

$$l_r = -\Phi_r/\beta + L \qquad (27)$$

where β is the phase constant of the feeders (assumed identical and lossless) and L is their mean length.

The relation between l_r and the dipole current distribution I_r follows directly from the circuit equations for a lossless transmission line and is,

$$V_0 = \left(\sum_{q=1}^{N} Z_{rq} I_q\right) \cos \beta l_r + jR_0 I_r \sin \beta l_r \qquad (28)$$

where V_0 is the common driving point voltage at the branch feeder junction, Z_{rq} the complex mutual impedance between dipoles r and q and R_0 the characteristic impedance of the feeders. Equation (28) applies to all branch feeders so that further manipulation (or alternatively the direct application of Thévenin's theorem to each feeder) yields the following linear matrix relationship,

$$[Z'_{rq}]\ [I_r] = [\sec \beta l_r] \qquad (29)$$

with $Z'_{rq} = Z_{rq}$ for $r \neq q$ and $Z'_{rq} = Z_{rr} + jR_0 \tan \beta l_r$ for $r = q$; V_0 has been normalized to unity. Equation (29) provides $2N$ real equations which determine the complex I_r resulting from N given feeder lengths. It follows that, with β real (lossless feeders), it is not possible in general to specify the amplitude and phase of I_r independently. This being so, any further adjustment of l_r from the value given by Equation (27) can only effect a compromise between amplitude and phase errors.

A suggested procedure for finding the best compromise is to use an optimizing computer programme for minimising the mean square of the vector errors $|I_r - \varepsilon^{j\Phi_r}|$ by repeated adjustments of l_r and L; an analytical solution is made extremely difficult because βl_r appears in transcendental form in Equation (29). The largest errors are to be expected at the ends of the array where the dipoles are not surrounded by other elements and also over those parts of the array where Φ_r is varying rapidly.

In the oscillatory null-filling solution, the largest phase-slope occurs at the ends of the array where the local impedance variation is also greatest and there is a possibility that the distribution errors caused by these two effects may tend to cancel with some dipole spacings. In the non-oscillatory null-filling solution, the largest phase variation occurs at the centre of the array where the mutual impedance effects are substantially uniform but the variation is augmented by the presence of the corrective differential phase step 2Δ. It is thought that the realization of the non-oscillatory solution in the presence of mutual coupling will yield rather greater mean square errors than those resulting from the alternative solution but this can be confirmed only by experiment.

We have already shown in connection with panel aerials (Section 4.2) that the null-filled v.r.p. remains satisfactory if the rate of variation of electrical phase over the array is reduced by partially realizing the synthesized distribution with element stagger. In principle, therefore, large steps in Φ_r can be eliminated from the actual phase distribution (approximated by l_r) if the appropriate dipole(s) are staggered horizontally. The "stagger" corresponds to the phase-steps (Equation (22)). The smoother phase distribution which results will be more amenable to accurate realization than the original distribution.

Finally, if the entire distribution is realized by staggering the dipoles of the array, then all branch feeders can be cut in length to an odd multiple of a quarter-wave and a constant-amplitude distribution is obtained independently of mutual coupling; this follows immediately from Equation (28) since in this base $\beta l_r = (2n - 1)\pi/2$ for all values of r. Computation has shown that null-filled v.r.p.s produced by stagger distributions derived from the synthesis solutions previously described are entirely satisfactory.

5.2. Random Phase Errors

The actual current distributions of null-filled arrays will be subject to phase errors from a number of sources. We have already discussed differential phase errors between array-halves (Section 4.1) and also errors due to inter-tier mutual coupling (Section 5.1); these phase errors are predictable and their effects on the v.r.p. can be calculated directly. A third source of error is the random variation of electrical length in the branch feeders due to cutting inaccuracies and also, to a minor extent, to the variation of feeder uniformity in manufacture.* In practice, the mean branch feeder length would be at least $N\lambda$ so that with $N = 20$ a cutting accuracy of $\pm 0{\cdot}1\%$ corresponds to a phase accuracy of $\pm 8{\cdot}5^\circ$ with conventional cables. It is not unreasonable to assume that a standard deviation of 10° could occur in the realization of the phase distributions; the accuracy of phase measurement at u.h.f. is comparable with this figure.

Random phase errors will either increase or decrease the null-filling of the synthesized v.r.p.s depending on the relative amplitude and phase of the contribution from the random errors at the null-points. Let us first consider a uniform (unperturbed) array of N sources fed with unit current and spaced $1{\cdot}0\lambda$ apart. A small phase error distribution ε_r (radians) produces an error pattern

$$j\sum_{r=1}^{N} \varepsilon_r \exp(j2\pi rk/N)$$

at the k^{th} null-point. If all the errors ε_r are independent and distributed normally with zero mean and standard deviation σ_ε** summation shows that the standard deviations of the real and imaginary components of this pattern are both equal to $\sigma_\varepsilon(N/2)^{1/2}$ for all values of k except at the central null-point, $k = N/2$, where only the imaginary component exists with standard deviation $\sigma_\varepsilon(N)^{1/2}$. The null-fillings due to phase errors, therefore, follow Rayleigh distributions except at the central null-point; the most probable amplitudes are $\sigma_\varepsilon(N/2)^{1/2}$ and there is a 50% probability that the amplitude exceeds $\sigma_\varepsilon(N \log 2)^{1/2}$. At the central null-point, the amplitude is distributed normally with a standard deviation $\sigma_\varepsilon(N)^{1/2}$.

In the presence of synthesized null-filling amplitudes g_k, the Rayleigh-distributed vectors and g_k add to give resultant amplitudes R_k with a distribution which has been given by Rice.[11] This distribution for R_k tends to a normal distribution for large null-filling amplitudes (more exactly, $\varepsilon_r << g_k$) and to the Rayleigh distribution for small null-filling amplitudes (i.e. $\varepsilon_r >> g_k$). In practice the normal distribution is approached at the null-points near the main lobe ($k \to 1$) and the Rayleigh distribution near the central null-point ($k \to N/2$). We may use Figs. 6 and 7 of Reference 11 by setting $a = g_k\sigma_\varepsilon(N/2)^{1/2}$ and $v = R_k\sigma_\varepsilon(N/2)^{1/2}$. At the central null-point, $g_{N/2}$ and the pattern error amplitude are approximately co-phased so that the resultant null-filling amplitude $R_{N/2}$ is distributed normally with mean $g_{N/2}$ and standard deviation $\sigma_\varepsilon(N)^{1/2}$.

As an example, consider a 20λ-array with nominal null-filling of 50% and random phase errors with standard deviations of 5° (0·087 radian) and 10° (0·175 radian). Table 1 gives the values of relative*** pattern amplitude at the null-points which have a 90% probability of being exceeded for these phase errors; the figures corresponding to zero phase errors are simply the intended relative null-filling amplitudes g_k/N with $N = 20$. Table 1 shows that, with small intended null-filling amplitudes ($k \to N/2$, $\sin\theta \to 0{\cdot}5$), the phase errors themselves are mainly responsible for the null-filling so that the resultant pattern is less likely to fall

---

* The statistical analysis in this Section is due to P. Knight.

** There is a 10% probability that $|\varepsilon_r| > 1{\cdot}64\sigma_\varepsilon$.

*** The amplitude of the main lobe is normalized to unity.

TABLE 1

Relative Pattern Amplitudes at the Null-points which have a 90% Probability of being exceeded with Phase Errors of Standard Deviation σ_ε

σ_ε	Relative pattern amplitude at null-points, × 10^3									
	$k =$ 1	2	3	4	5	6	7	8	9	10
0	159	80	53	40	32	27	23	20	18	16
5°	142	63	38	25	19	15	13	11	10	4
10°	127	50	30	22	18	17	17	17	17	5

below the intended amplitudes; the effect is more marked with large phase errors.

The conclusion is that the reduction of null-filling amplitudes from their specified values by random phase errors in the actual current distribution must be taken into account when drawing up the null-filling specification g_k to be used for synthesis.

6. FINAL REMARKS AND CONCLUSIONS

Methods have been described for synthesizing approximate cosecant radiation patterns by perturbing the phases of the currents in a constant amplitude linear array of equispaced elements. The methods involve the synthesis of a symmetrical pattern in phase quadrature with the primary pattern of the unperturbed array. This quadrature pattern is made to satisfy the required cosecant amplitudes at the null-points of the primary pattern; it then fills the nulls between the side-lobes of the primary pattern to a degree corresponding to the cosecant specification. The constant amplitude condition is then imposed on the array currents and the phase distribution readjusted to allow for the change in the primary pattern which results.

Procedures have been given in Section 3.2 for deriving the uncorrected symmetrical phase distributions which provide null-filling quadrature patterns. There are two solutions available and they depend on the choice of polarities in the cosecant amplitude specification. In the non-oscillatory solution (Section 3.3), all specified amplitudes are given identical polarities and the phase adjustment simply involves a differential phase shift between array-halves. In the oscillatory solution (Section 3.4), consecutive specified amplitudes are made to alternate in polarity; in this case, primary pattern correction is effected by perturbing the phase distribution with a small shift which alternates in polarity over consecutive elements of the array. The two solutions are related in that the uncorrected phase distribution of one is the inverse of the other (Section 3.5). Provided the degree of null-filling is limited to about 50%, the corrective phase adjustments require no further iteration.

These techniques may be directly applied to the problem of null-filling the v.r.p.s of v.h.f. and u.h.f. transmitting aerials by weighting the cosecant amplitude specification inversely with the v.r.p. of a single tier (Section 4.1). With panel aerials, however, the phase distribution must be split into identical blocks. Two solutions have been given (Section 4.2). In the multiplicative method, the panel v.r.p. is itself null-filled prior to null-filling the v.r.p. of the array of panels, whereas in the panel-tilt solution element-stagger and electrical phase shift are employed to enable co-phased panels to be used. The gain reduction of an aerial providing a 50% null-filled v.r.p. is unlikely to exceed 0·4 dB and the cosecant specification is typically satisfied over a frequency bandwidth of ±10%.

Some practical difficulties may be encountered in the actual realization of the prescribed phase distributions; the main causes are inter-tier mutual coupling and random phase errors originating in the branch feeders of the aerial. Where mutual coupling cannot be ignored, the feeder lengths should be re-adjusted to reduce the errors in the actual current distribution to the point where the resulting v.r.p. becomes acceptable. Random phase errors, in general, are likely to reduce the null-filling amplitudes; they are best allowed for by increasing the specified null-filling amplitudes before synthesis so that the final v.r.p. has sufficient latitude to meet the intended specification in the presence of the estimated phase errors.

The main conclusions reached in the report are as follows. Of the two methods described for null-filling v.r.p.s by phase perturbation, the non-oscillatory solution yields rather better results, in general, than the alternative solution, although the actual advantage depends to some extent upon the desired beam-tilt. For special applications the symmetry of the null-filled v.r.p.s given by the oscillatory solution may be of some advantage; in the multiplicative method for null-filling the v.r.p.s of panel aerials this characteristic is essential. Another minor advantage of the oscillatory solution is that the largest phase slopes occur at the extremities of the array rather than at its centre and this may be more amenable to actual realization.

With simple aerials the two solutions exhibit almost identical gain reductions but, with the oscillatory solution, the null-filling is maintained over a smaller bandwidth because the v.r.p. only just meets the specification (for large angles from the horizontal) at the centre-frequency. The reflexion coefficient of the aerial at the main feeder is normally smaller with the non-oscillatory solution but both solutions give comparable figures for aerial mismatch with large departures from the centre-frequency.

With panel aerials, the panel-tilt method of synthesis is more accurate than the multiplicative method as the latter gives rather poor results near the half-period point in the v.r.p. of the array of panels. Either null-filling solution may be used with the panel-tilt method; the differences in gain reduction and reflexion coefficient are negligible. With the non-oscillatory solution the null-filling is again maintained over a slightly greater bandwidth but if the oscillatory solution is employed the panel-tilt may be restricted to just one extremity of the array. Moreover, if we use a lagging, rather than a leading, quadrature distribution this tilt appears at the bottom of the aerial and the tilted panel(s) point downwards away from the array; this would probably make it easier to achieve the required current distribution in the presence of mutual coupling between panels. In the non-oscillatory solution the central pair(s) of panels are tilted and either incline towards their respective array-halves (leading quadrature) or towards each other (lagging quadrature), both arrangements giving large mutual coupling.

Finally, it is emphasized that the great advantage of null-filling the v.r.p.s of v.h.f. and u.h.f. aerials by phase perturbation lies in the fact that the constant amplitude distribution can be realized in most cases by simply cutting the branch feeders to the aerial elements to the prescribed phase distribution; if mutual coupling makes this realization difficult, entirely satisfactory patterns can be obtained by employing mechanical stagger instead. The methods of synthesis given here are straigthforward and easy to use in practice.

7. REFERENCES

1. Considerations affecting the aperture and beam-tilt of u.h.f. transmitting aerials. Research Department Report No. E-099, Serial No. 1964/20.

2. See for example, LEE, Y.W. 1960. Statistical theory of communication. (New York, Wiley, 1960. Chap. 2, p. 11).

3. WOODWARD, P.M. *and* LAWSON, J.D. 1948. The theoretical precision with which an arbitrary radiation pattern may be obtained from a source of finite size. *J.Instn elect.Engrs.*, 1948, **95**, III, 37, pp. 363 - 370.

4. WOODWARD, P.M. 1946. A method of calculating the field over a plane aperture required to produce a given polar diagram. *J.Instn elect. Engrs.*, 1946, **93**, IIIA, 10, pp. 1554 - 1558.

5. HARRIS, J.H. *and* SHANKS, H.E. 1961. A method for synthesis of optimum directional patterns from non-planar apertures. *I.R.E. Trans. Antennas Propag.*, 1962, **AP-10**, 3, pp. 228 - 236.

6. RHODES, D.R. 1963. The optimum line source for the best mean-square approximation to a given radiation pattern. *I.E.E. Trans.Antennas Propag.*, 1963, **AP-11**, 4, pp. 440 - 446.

7. PROCTOR, E.K. *and* ABLOW, C.M. 1962. A variational method of synthesizing antenna power patterns. *JORDAN, E.C. ed. Electromagnetic theory and antennas. Part 2,* New York, Macmillan, 1963, pp. 1225 - 1228.

8. DUNBAR, A.S. 1952. On the theory of beam shaping. *J. appl. Phys.*, 1952, **23**, pp. 847 - 853.

9. SHANKS, H.E. 1960. A geometrical optics method of pattern synthesis for linear arrays. *I.R.E. Trans. Antennas Propag.*, 1960, **AP-8**, 5, pp. 485 - 490.

10. SHONE, A.B. *and* WHARTON, W. 1962. Transmitter combining networks for television transmitting stations. *Institution of Electrical Engineers, Television Engineering,* London, I.E.E., 1963, pp. 462 - 472.

11. RICE, S.O. 1945. Mathematical analysis of random noise. *Bell Syst.tech.J.*, 1945, **24**, 1, pp. 46 - 156.

8. APPENDIX

Differential phase correction of the non-oscillatory solution

We are considering an array of N(even) isotropic sources spaced $1{\cdot}0\lambda$ apart fed with currents of unit amplitude and phases $\phi_r + \Delta$ for the top half-array and phases $\phi_r - \Delta$ for the bottom half-array, i.e. ϕ_r is the symmetrical phase distribution synthesized from the quadrature pattern and 2Δ is the corrective differential phase shift. The radiation pattern $p(\sin\theta)$ of the array is the sum of the half-array patterns:

$$p(\sin\theta) = \sum_{r=1}^{N/2} \varepsilon^{j(\phi_r + \Delta)} \varepsilon^{-j(\overline{2r-1}\pi\sin\theta)}$$

$$+ \sum_{r=1}^{N/2} \varepsilon^{j(\phi_r - \Delta)} \varepsilon^{j(\overline{2r-1}\pi\sin\theta)}$$

$$= 2\sum_{r=1}^{N/2} \varepsilon^{j\phi_r} \cos(\overline{2r-1}\pi\sin\theta - \Delta) \qquad (30)$$

Suppose now that ϕ_r is small enough to enable us to write $\cos\phi_r = 1 - \phi_r^2/2$ and $\sin\phi_r = \phi_r$, also that Δ is sufficiently small for the approximations $\cos\Delta = 1$ and $\sin\Delta = \Delta$ to be valid. Equation (30) may then be rewritten as follows:

$$p(\sin\theta) = 2\sum_{r=1}^{N/2} \{1 - \frac{\phi_r^2}{2} + j\phi_r\}\{\cos(\overline{2r-1}\pi\sin\theta)$$

$$+ \Delta\sin(\overline{2r-1}\pi\sin\theta)\}$$

The primary (in phase) component of this pattern is given by

$$\text{Re}\, p(\sin\theta) =$$

$$2\sum_{r=1}^{N/2}\{\cos(\overline{2r-1}\pi\sin\theta) - \frac{\phi_r^2}{2}\cos(\overline{2r-1}\pi\sin\theta)$$

$$+ \Delta\sin(\overline{2r-1}\pi\sin\theta)\}$$

which on summation gives,

$$\text{Re}\, p(\sin\theta) = p_0(\sin\theta) - \sum_{r=1}^{N/2}\phi_r^2\cos(\overline{2r-1}\pi\sin\theta)$$

$$+ 2\Delta\frac{\sin^2(\frac{N}{2}\pi\sin\theta)}{\sin(\pi\sin\theta)} \qquad (31)$$

In Equation (31) the first term is the pattern of the unperturbed array (Equation (5)), the second term is the primary error pattern introduced by the null-filling phase distribution ϕ_r and the third term is the component due to differential phase 2Δ; the third order term has been dropped. The component patterns in Equation (31) have been approximately drawn in Fig. 9 for $N = 12$.

The error pattern has most effect on Re $p(\sin\theta)$ over the range $0 < \sin\theta < 0{\cdot}25$ (see Fig. 8 for example) so that the differential phase term is required to reduce the error by as much as possible over that range. Tentatively, we equate the mean of the differential phase term (approximately equal to one half of its envelope amplitude) to the error pattern at $\sin\theta = 5/2N$ for optimum correction,* i.e.

$$\sum_{r=1}^{N/2}\phi_r^2\cos(\overline{2r-1}\;5\pi/2N) \simeq \Delta\;\text{cosec}(5\pi/2N) \qquad (32)$$

It is recalled that in the non-oscillatory solution, the largest phase perturbations ϕ_r are given to those pairs of elements near the centre of the array. For uniform null-filling (m fixed over range $0 < \sin\theta < 0{\cdot}5$) we find that $\phi_1^2 >> \phi_2^2, \phi_3^2, \ldots . \phi_{N/2}^2$. In these cases, therefore, there is little error in including only the $r = 1$ term in the summation of Equation (32); the approximate expression for determining the optimum value of Δ is:

$$\Delta \simeq \tfrac{1}{2}\phi_1^2\sin(5\pi/N) \qquad (33)$$

Equation (33) will become inaccurate for small values of N.

---

* Trial correction with $N = 20$ gave optimum results by equating these terms at the point $\sin\theta = 0{\cdot}125$.

SMW

Printed by BBC Research Department, Kingswood Warren, Tadworth, Surrey